

TopoBench: A Framework for Benchmarking Topological Deep Learning

Lev Telyatnikov^{*1}, Guillermo Bernárdez^{*2}, Marco Montagna¹, Mustafa Hajij³, Martin Carrasco⁴, Pavlo Vasylenko⁵, Mathilde Papillon², Ghada Zamzmi⁶, Michael T. Schaub⁷, Jonas Verhellen⁸, Pavel Snopov⁹, Bertran Miquel-Oliver^{10,11}, Manel Gil-Sorribes¹², Alexis Molina¹², Victor Guallar^{10,13}, Theodore Long¹⁴, Julian Suk¹⁵, Patryk Rygiel¹⁵, Alexander Nikitin¹⁶, Giordan Escalona¹⁷, Michael Banf¹⁸, Dominik Filipiak^{19,18}, Max Schattauer¹⁸, Liliya Imasheva¹⁸, Alvaro Martinez²⁰, Halley Fritze²¹, Marissa Masden²², Valentina Sánchez²³, Manuel Lecha²⁴, Andrea Cavallo²⁵, Claudio Battiloro²⁶, Matt Piekenbrock²⁷, Mauricio Tec²⁶, George Dasoulas²⁶, Nina Miolane², Simone Scardapane¹, Theodore Papamarkou²⁸

¹Sapienza University of Rome, ²UC Santa Barbara, ³VU Amsterdam, ⁴University of Fribourg, ⁵Instituto Superior Técnico, ⁶University of South Florida, ⁷RWTH Aachen University, ⁸University of Copenhagen, ⁹University of Texas Rio Grande Valley ¹⁰Barcelona Supercomputing Center, ¹¹Universitat Politècnica de Catalunya, ¹²Nostrum Biodiscovery, ¹³Catalan Institution for Research and Advanced Studies, ¹⁴Atalaya Capital Management, ¹⁵University of Twente, ¹⁶Aalto University, ¹⁷University of Rochester, ¹⁸Perelyn GmbH, ¹⁹Adam Mickiewicz University, ²⁰Columbia University, ²¹University of Oregon, ²²University of Puget Sound, ²³Tilburg University, ²⁴Istituto Italiano di Tecnologia, ²⁵Delft University of Technology, ²⁶Harvard University, ²⁷Northeastern University, ²⁸PolyShape

Reviewed on OpenReview: <https://openreview.net/forum?id=07sTzyEVtY>

Editor: Yi Liu

Abstract

This work introduces **TopoBench**, an open-source library designed to standardize benchmarking and accelerate research in topological deep learning (TDL). **TopoBench** decomposes TDL into a sequence of independent modules for data generation, loading, transforming and processing, as well as model training, optimization and evaluation. This modular organization provides flexibility for modifications and facilitates the adaptation and optimization of various TDL pipelines. A key feature of **TopoBench** is its support for transformations and lifting across topological domains. Mapping the topology and features of a graph to higher-order topological domains, such as simplicial and cell complexes, enables richer data representations and more fine-grained analyses. The applicability of **TopoBench** is demonstrated by benchmarking several TDL architectures across diverse tasks and datasets.

Keywords: Benchmark, topological deep learning, topological neural networks.

* Equal contribution.

1 Introduction

In geometric deep learning (GDL; Bronstein et al., 2021), graph neural networks (GNNs; Zhou et al., 2020) have demonstrated impressive capabilities in processing relational data represented as graphs. However, because graphs represent relationships through edges, they inherently capture only pairwise interactions, which can be a limiting factor. For example, social interactions often involve groups of individuals rather than just pairs, and electrostatic interactions in proteins can span multiple atoms. Topological deep learning (TDL; Papamarkou et al., 2024; Bodnar, 2023; Hajij et al., 2023b; Papillon et al., 2023) offers a framework for modeling complex systems characterized by such multi-way relations among components, leveraging to that end higher-order discrete topological domains (such as simplicial and cell complexes, see Section 2). Topological neural networks (TNNs; Feng et al., 2019; Bunch et al., 2020; Hajij et al., 2020; Bodnar et al., 2021a; Ebli et al., 2020; Schaub et al., 2021; Bodnar et al., 2021b; Chien et al., 2021), which are part of TDL, have found applications in numerous fields that involve higher-order relational data such as social networks (Knoke and Yang, 2019), protein biology (Jha et al., 2022), physics (Wei and Fink, 2024), and computer networks (Bernárdez et al., 2025). TNNs have also shown their potential in various machine learning tasks (Dong et al., 2020; Barbarossa and Sardellitti, 2020; Chen et al., 2022; Roddenberry et al., 2021; Telyatnikov et al., 2025; Giusti et al., 2023).

However, as identified in a recent position paper (Papamarkou et al., 2024), the rapid growth of TDL research has introduced challenges in ensuring reproducibility and conducting systematic comparative evaluations of TNNs. To address these challenges, this work introduces **TopoBench**¹, an open-source and modular framework for TDL. By providing a comprehensive pipeline –from data integration and processing to modeling and evaluation–, our proposed framework facilitates both development and benchmarking of TNNs (Figure 1 illustrates the overall workflow). More specifically, **TopoBench** directly addresses the following relevant limitations of current TDL models’ evaluations (Papamarkou et al., 2024):

Data availability: Although many complex systems exhibit higher-order interactions, they are mostly collected in the form of point clouds or graphs, implying the failure to fully capture a more nuanced interplay. For instance, in a social network, we might track friendships between individuals but overlook whether they belong to the same group, losing valuable higher-order relationships. This limitation arises because current experimental designs often impose constraints on what data can be collected, making it difficult to systematically capture complex, multi-level relationships. **TopoBench** mitigates the scarcity of higher-order data in three ways. First, it provides an interface for uploading publicly available higher-order datasets. Second, it facilitates the loading of user-defined datasets – whether higher-order or not. Third, it implements lifting algorithms (i.e. mappings between different discrete topological domains) to automate the construction of new topological datasets.

Standardization: There is a broad spectrum of TNNs in the TDL literature, each using distinct techniques to preprocess and encode data within a specific higher-order topological domain. This diversity complicates performance comparisons between models on different datasets. To address this issue, **TopoBench** implements a unifying pipeline for data preprocessing and predictive performance evaluation metrics.

1. <https://github.com/geometric-intelligence/TopoBench>

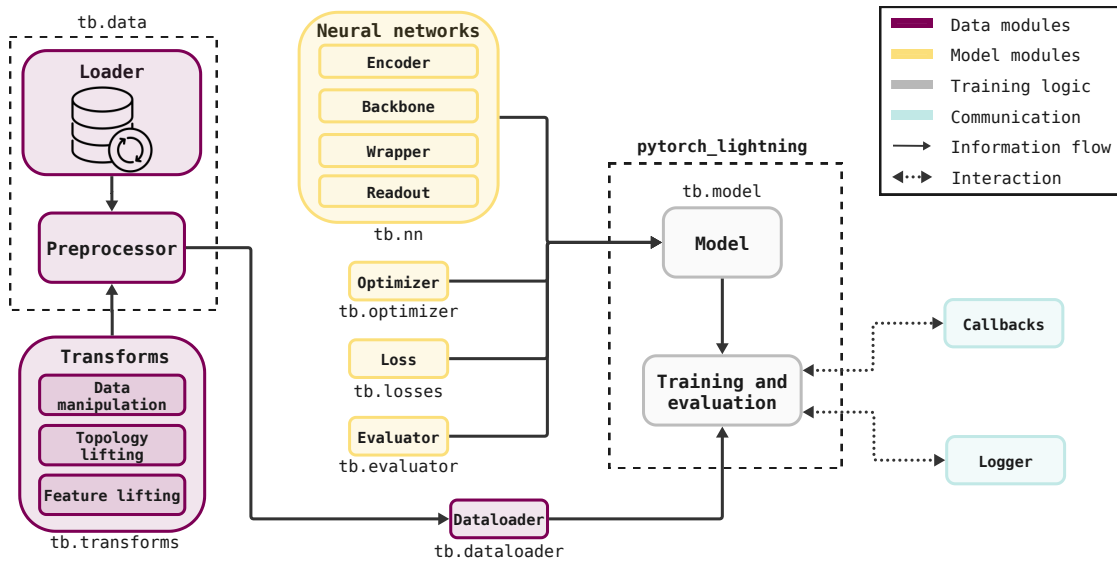


Figure 1: Workflow of TopoBench, consisting of four main components: data modules, model modules, training modules, and communication modules.

Benchmarking: The described challenges collectively impede the establishment of standardized benchmarking practices within the TDL community. This work provides the first cross-domain benchmarking of TNNs across diverse datasets, adhering to a well-established and rigorous machine learning pipeline. Furthermore, TopoBench ensures the complete reproducibility of the experiments.

Democratization of TDL: The emerging nature of TDL, coupled with its reliance on advanced mathematical and computer science expertise, poses a barrier to broader adoption. TopoBench democratizes TDL by automating and modularizing the pipeline, offering a high-level interface to simplify coding, facilitating seamless integration through a modular design, and ensuring complete compatibility with the PyTorch ecosystem. It provides an accessible testbed for newcomers to experiment with topological domains, models, and datasets, fostering innovation and expanding the scope of TDL applications.

The remainder of this paper is structured as follows: Section 2 introduces key TDL concepts –with technical details in the appendix. Section 3 provides a review of related software. Section 4 details TopoBench’s modules and functionality. Section 5 demonstrates TopoBench through benchmarking experiments. Section 6 concludes with remarks and future directions.

2 Background

This section aims to build the general intuition necessary to understand TopoBench, while providing references to its formal mathematical foundations.

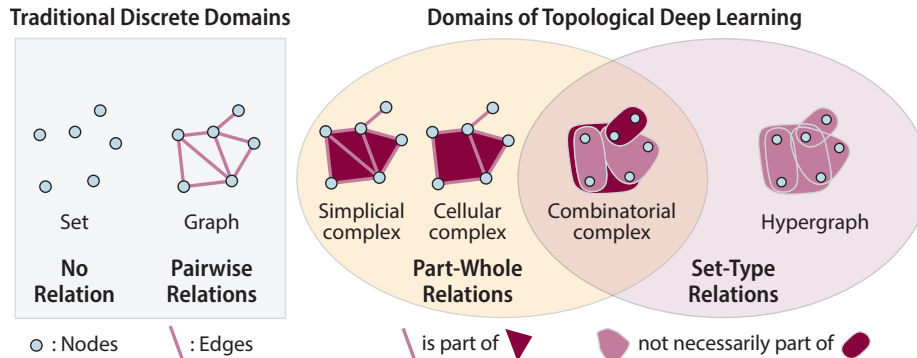


Figure 2: Topological Deep Learning Domains. Nodes in blue, (hyper)edges in pink, and faces in dark red. Figure adapted from Papillon et al. (2023).

Topological domains. Relational data can be represented in various forms, with graph representation being the most common framework. However, as discussed in the Introduction, graphs are limited to pairwise relations. TDL methodologies overcome this constraint by encoding higher-order relationships through combinatorial and algebraic topology concepts. Fig. 2 illustrates the standard discrete, higher-order topological spaces used to that end, which enable more complex relational representations via part-whole and set-types relations (Papillon et al., 2023); see Appendix A.1 for the formal definition of each of these topological domains.

Liftings. Since most relational data is traditionally collected in discrete domains, such as point clouds and graphs, transitioning to richer topological representations requires mappings between domains — for instance, from a graph to a simplicial complex. This process of mapping, known as lifting, enables more flexible and expressive data representations (further details in Section 4.3 and Appendix A.2).

Topological neural networks. Once the data is represented within a chosen topological domain, the TDL pipeline employs neural networks specifically designed for that domain. These models process higher-order structures, leveraging specialized inductive biases. Such networks, referred to as Topological Neural Networks (TNNs), enable learning directly from data represented through topological domains (see Appendix A.3). In general, TNNs exploit a higher-order message-passing mechanism (see Appendix A.5), which generalizes the traditional graph-based message-passing approach (see Appendix A.4), allowing for more comprehensive information propagation through higher-order structures.

3 Existing Software

Graph-based learning and GDL are supported by several software packages, including `NetworkX` (Hagberg et al., 2008), `KarateClub` (Rozemberczki et al., 2020), `PyG` (Fey and Lenssen, 2019), `DGL` (Wang et al., 2019), and `Open Graph Benchmark` (OGB; Hu et al., 2020, 2021). `NetworkX` enables computations on graphs, while `KarateClub` implements unsupervised learning algorithms for graph-structured data. `PyG` and `DGL` provide functionality for GDL as well as standard graph-based learning. Lastly, OGB provides a collection of

graph datasets and a benchmarking framework that supports reproducible graph machine learning research; however, it does not address TDL-specific needs.

Various tools also exist for higher-order domains. For hypergraphs, simplicial complexes, and other topological structures, **HyperNetX** (Liu et al., 2021), **XGI** (Landry et al., 2023), **DHG** (Feng et al., 2019), and **TopoX** (Hajij et al., 2024) each focus on different facets. **HyperNetX** facilitates hypergraph computations, whereas **XGI** supports both hypergraphs and simplicial complexes. **DHG** implements deep learning algorithms for graphs and hypergraphs. **TopoX** is a suite of three packages—**TopoNetX**, **TopoEmbedX**, and **TopoModelX**—that provide broader support for hypergraphs, simplicial, cellular, path, and combinatorial complexes (Hajij et al., 2023a). **TopoNetX** facilitates constructing and computing on these domains, including working with nodes, edges, and higher-order cells; **TopoEmbedX** embeds higher-order domains into Euclidean spaces, while **TopoModelX** implements most TNNs surveyed in Papillon et al. (2023).

Additionally, topological data analysis (TDA) libraries such as **GUDHI** (The GUDHI Project, 2015), **giotto-tda** (Tauzin et al., 2021), and **scikit-tda** (Nathaniel Saul, 2019) offer robust tools for topological computations, like persistent homology diagrams and topological invariant metrics. These TDA packages can provide valuable building blocks to extract topological information from data within TDL pipelines.

TopoBench Contextualization

TopoBench leverages and extends this existing software ecosystem to provide a unified benchmarking infrastructure for TDL. The framework directly integrates established libraries including **NetworkX** for graph computations and the **TopoX** suite—**TopoNetX** for higher-order structure construction and **TopoModelX** for TNN implementations. **TopoBench** also incorporates graph-based models from **PyG** and enables seamless integration of models from original research repositories, providing unprecedented flexibility for TDL evaluation.

While these existing packages provide essential building blocks, **TopoBench** introduces novel capabilities that address critical gaps in the TDL software ecosystem. Unlike **OGB**’s focus on graph learning, **TopoBench** provides comprehensive data management for topological domains, including automated dataset downloading, storage, and processing capabilities. The framework introduces automated lifting transformations that extend beyond **TopoNetX**’s manual construction capabilities, enabling seamless data connectivity transformations between topological domains with integrated feature handling. Additionally, **TopoBench** offers unified mini-batching across all topological structures through a shared dataloader and streamlined configuration systems for experiment setup—capabilities absent from current TDL software.

These innovations collectively establish **TopoBench** as the first comprehensive benchmarking framework for TDL. The framework’s unified data representation enables consistent treatment of diverse topological structures, allowing researchers to evaluate models across different domains using standardized procedures. This approach transforms the fragmented TDL software landscape into a cohesive research environment, providing the reproducible benchmarking infrastructure that the rapidly evolving field requires.

Algorithm 1 Execution pipeline for model training in TopoBench

```

1: Input: General cfg configuration file
2: dataset  $\leftarrow$  Loader(cfg.dataset) # Dataset loading
3: splits  $\leftarrow$  PreProcessor(dataset, cfg.transforms) # Transforms and splits
4: dataloader  $\leftarrow$  Dataloader(dataset) # Batch generator
5: model  $\leftarrow$  Model # Model initialization
6:   nn.Encoder(cfg.model),
7:   nn.Backbone(cfg.model),
8:   nn.BackboneWrapper(cfg.model),
9:   nn.Readout(cfg.model),
10:  *[Evaluator(cfg.evaluator), Optimizer(cfg.optimizer), Loss(cfg.loss)]
11: )
12: trainer  $\leftarrow$  lightning.Trainer(cfg.trainer, cfg.callbacks, cfg.logger)

12: Model training:
13: trainer.fit(model, dataloader) # Model training

14: Model step for each batch:
15: batch  $\leftarrow$  self.encoder(batch) # Feature encoder
16: model_out  $\leftarrow$  self.forward(batch) # TNN
17: model_out  $\leftarrow$  self.readout(model_out, batch) # Readout
18: model_out  $\leftarrow$  self.loss(model_out, batch) # Loss computation
19: self.evaluator.update(model_out) # Evaluator update

```

4 The TopoBench Library: Module Outline, Datasets and Liftings

TopoBench implements a unified and flexible workflow that facilitates the addition of new datasets, data manipulation and preprocessing methods (collectively referred to as transforms), deep learning models, as well as custom metrics and losses. This design ensures applicability across a wide range of tasks and enables a broad cross-domain comparison, currently lacking in the TDL literature. Each module within TopoBench is assigned a distinct role while maintaining a consistent input-output structure, which provides a modular interface across all topological domains. Figure 1 outlines the TopoBench modules, grouped by functionality into data, model, training, and communication components. Algorithm 1 illustrates the TopoBench execution pipeline in pseudo-code.

4.1 TopoBench Modules

Data modules. These modules manage and process data within TopoBench, including `Loader`, `Transforms`, `PreProcessor`, and `Dataloader`.

Loader. The `Loader` module provides an interface for downloading and storing data, built upon the widely adopted `InMemoryDataset` from PyG, enhancing interoperability. The project webpage offers detailed tutorials on the library, including a step-by-step guide to integrating customized data with these interfaces.

Transforms. `Transforms` modules are implemented as subclasses of `BaseTransform` (provided by `PyG`) and include three categories: data manipulation, topology lifting, and feature lifting. The data manipulation module enables general data transformations (e.g., adapting `PyG` (Fey and Lenssen, 2019) or `TopoX` (Hajij et al., 2024) transforms for use in `TopoBench`). The topology lifting and feature lifting modules handle the conversion of data from one topological domain to another (see Section 4.3). Each transform accepts a `Data` object as input, performs the necessary computations, and outputs the modified `Data` object. These composable operators can be easily customized for various tasks.

Pre-processor. The `PreProcessor` class applies a sequence of transforms to a dataset. It accepts a dataset object and a list of transforms, iterating over the dataset to apply each transform in turn. To avoid re-computing the same transforms repeatedly, the preprocessed dataset is saved in a dedicated folder for each transform configuration. This setup ensures that each dataset is processed only once per configuration, mitigating the potentially time-consuming nature of preprocessing large datasets. `PreProcessor` also generates or loads data splits according to a chosen strategy (e.g., random splits with predefined proportions, k-fold cross-validation, or fixed splits).

Dataloader. The `DataLoader` module provides a consistent interface for batch training across graphs, hypergraphs, simplicial complexes, cell complexes, and combinatorial complexes. By supporting mini-batching for all these domains, it helps make training more tractable on large datasets.

Model modules. The neural network modules form the core of the modeling pipeline. The `encoder` component maps initial data features into a latent space and applies a learnable transformation before passing the data to a TNN model –thus standardizing the input across all models. The `backbone` TNN can be imported from existing PyTorch libraries (e.g., `TopoX` or `PyG`), or built on a custom basis within `TopoBench` (see Table 10 in Appendix C). The `wrapper` ensures the correct input is provided to the forward pass of the `backbone` TNN model and collects the output in a dictionary. This design streamlines input and output handling across different topological domains, making it easier to integrate new models into `TopoBench`.

The `readout` module converts latent representations from the neural network into final predictions. The `Loss` module defines a loss function (from the `PyTorch` library, or customized), while the `Optimizer` module configures the optimizer and scheduler. This design allows seamless use of any optimizer and scheduler from `torch.optim`, thereby supporting flexible and robust training. Finally, the `evaluator` module, built upon `torchmetrics`, provides metrics for both classification and regression tasks –while also allowing for tailored ones for specific datasets and tasks. Notably, the flexibility of these modules enable researchers to implement topology-specific evaluation criteria as needed for their particular applications.

Training and communication modules. The `Model` class defines a training pipeline for all domains (see lines 14–19 of Algorithm 1). Inheriting from `LightningModule`, it requires `Encoder`, `Wrapper`, `Backbone`, `Readout`, `Evaluator`, `Loss`, and `Optimizer` objects as inputs. The `lightning.Trainer` then automates training, evaluation, and testing. Additional functionalities can be incorporated via callbacks, and users can monitor training with various loggers (e.g., wandb, tensorboard). Both are standard tools in `Lightning` and are referred to as communication modules in `TopoBench`.

4.2 Datasets

TopoBench includes a wide selection of datasets to accommodate both standard graph-based and higher-order domains. It is the first framework to enable the creation of reliable, reproducible higher-order datasets through the use of various lifting mappings. A subset of these datasets are also used in the experiments of Section 5 for demonstration purposes. See Appendix C.3 for descriptive statistics of the datasets.

Graph-based datasets. A number of well-known datasets commonly used in graph-based learning are supported. Citation networks such as Cora, Citeseer, and PubMed (Yang et al., 2016) are included, along with heterophilous datasets (where nodes connected by an edge predominantly belong to different categorical classes), such as Amazon Ratings, Roman Empire, Minesweeper, Tolokers, and Questions. The TU datasets, including MUTAG, PROTEINS, NCI1, NCI109, IMDB-BIN, IMDB-MUL, and REDDIT (Morris et al., 2020), are also integrated, as are molecule datasets like ZINC (Gómez-Bombarelli et al., 2018) and AQSOL (Dwivedi et al., 2023). Furthermore, TopoBench supports the US County Demographics dataset (Jia and Benson, 2020), illustrating its adaptability to various graph structures.

Datasets with higher-order interactions. Several datasets with higher-order interactions are included in TopoBench, showcasing its capabilities to handle data supported on hypergraphs, simplicial complexes, and other topological domains. The MANTRA dataset (Ballester et al., 2024) is part of TopoBench, offering over 43,138 two-dimensional and 249,000 three-dimensional triangulations of surfaces and manifolds, which can be used, for example, as features on a simplicial complex. In addition, the widely used AllSet hypergraph datasets (Chien et al., 2021)—Cora-Cocitation, Citeseer-Cocitation, PubMed-Cocitation, Cora-Coauthorship, and DBLP-Coauthorship—are integrated, following the same preprocessing as HyperGCN (Yadati et al., 2019). These hypergraphs group documents co-authored or co-cited together into single hyperedges. Collectively, these examples illustrate how TopoBench supports data beyond traditional graph pairwise interactions.

Compatibility and custom datasets. To simplify dataset integration, TopoBench provides convenient wrappers that build on PyG loaders (e.g., TUDatasets, Planetoid, ZINC). In many cases, these wrappers enable straightforward use of any graph dataset already supported by PyTorch Geometric, as well as newly introduced datasets such as MANTRA, the hypergraph citation networks, and Human3.6m. Support for custom datasets is facilitated by a simple interface with two key methods: `download()`, for fetching or extracting raw files, and `process()`, for converting the data into the desired relational structure (graph, hypergraph, simplicial or cell complex). Code examples and tutorials provided in TopoBench illustrate the TopoBench interface for loading custom user-defined datasets². This approach guarantees users can easily extend TopoBench to any dataset of interest, thus maintaining the library’s modular and extensible design.

4.3 Topological Liftings

In the context of TDL, as outlined in Section 2, liftings facilitate the mapping of data from one topological representation to another. This mapping comprises two key aspects:

2. https://github.com/geometric-intelligence/TopoBench/blob/main/tutorials/tutorial_add_custom_dataset.ipynb

structural lifting and *feature lifting* (see Figure 3 for a visual example, and a formal definition can be found in Appendix A.2). Informally, the *structural lifting* is responsible for the transformation of the underlying relationships or elements of the data. For instance, it might determine how nodes and edges in a graph are mapped into triangles and tetrahedra in a simplicial complex. This structural transformation can be further categorized into *connectivity-based*, where the mapping relies solely on the existing connections within the data, and *feature-based*, where the data’s inherent properties or features guide or even fully determine the new structure. Feature lifting, conversely, addresses the transfer of data attributes or features during mapping, ensuring that the properties associated with the data elements are consistently preserved in the new representation, thus maintaining information integrity. Both structural and feature liftings are crucial for the effective application of TDL to diverse and complex datasets.

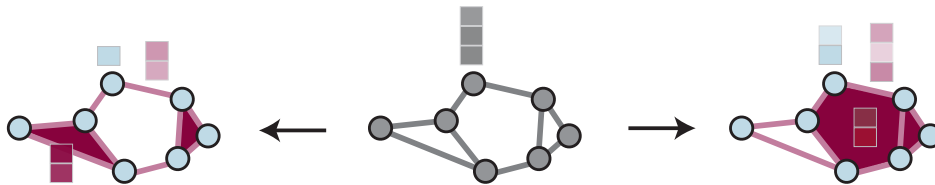


Figure 3: An illustration of lifting a graph (center) to two different topological domains: a simplicial complex (left) and a cell complex (right). The structural lifting maps the nodes and edges of the graph to higher-order topological structures, such as faces, while the feature lifting ensures the associated feature functions are consistently transferred between domains.

Table 3 in Appendix B provides a comprehensive list of all the liftings currently implemented in **TopoBench**. Currently, **TopoBench** supports 11 structural liftings targeting simplicial complexes; 2 targeting cell complexes; 10 moving to hypergraphs; and 3 from a domain to combinatorial complexes. Notably, **TopoBench**’s modular design simplifies the integration of additional liftings, ensuring the framework’s adaptability to evolving research needs.

5 Numerical Experiments

This section presents numerical experiments that illustrate the breadth of **TopoBench**’s functionality by performing a cross-domain comparison. The overall setup is first described, then results from benchmarking various graph, hypergraph, and TNNs are reported, and an ablation study on signal propagation is presented to demonstrate how **TopoBench** supports comparisons in TDL.

5.1 Setup

Learning tasks and datasets. Four types of tasks are considered: node classification (seven datasets), node regression (seven datasets), graph classification (seven datasets), and graph regression (one dataset). For node classification, the cocitation datasets (Cora,

Citeseer, and PubMed) and heterophilic datasets (Amazon Ratings, Minesweeper, Roman Empire, and Tolokers) are used (Platonov et al., 2023). For node regression, the election, bachelor, birth, death, income, migration, and unemployment datasets from US election map networks are adapted (Jia and Benson, 2020). In these datasets, each node represents a US state, edges connect neighboring states, and each state is characterized by demographic and election statistics. For each dataset, one statistic is designated as the target, while the others serve as node features, with the dataset named for the chosen target statistic. For graph classification, the TUDataset collection is used, specifically MUTAG, PROTEINS, NCI1, NCI109, IMDB-BIN, IMDB-MUL, and REDDIT (Morris et al., 2020). For graph regression, the ZINC dataset is employed (Irwin et al., 2012).

Higher-order datasets are constructed by lifting these graph datasets. For demonstration purposes, one structural lifting is considered for each of the considered higher-order topological spaces: cycle-based lifting for the cell domain (see Example 5), clique complex lifting for the simplicial domain (see Example 6), and k -hop lifting for the hypergraph domain (see Example 8). As for the feature lifting, the projected sum is always considered in all of these scenarios. Descriptive statistics for these topological versions of the datasets are provided in Table 4 in Appendix C.3.

Models. Twelve neural networks, supported across four domains (graphs, hypergraphs, simplicial complexes, and cell complexes), are benchmarked. These include three GNNs (GCN, GIN, and GAT), three hypergraph neural networks (EDGNN, AllSetTransformer, and UniGNN2), three simplicial neural networks (SCN, SCCN, and SCCNN), and three cell complex neural networks (CCXN, CWN, and CCCN). Details on these architectures and their hyperparameters appear in Appendix C. In particular, the number of learnable parameters for each best model configuration can be found in Table 8, while the corresponding runtimes are provided in Table 9.

Training and evaluation. Five splits are generated for each dataset, with 50%/25%/25% of the data going to the training, validation, and test sets, respectively; the exception is ZINC, for which the predefined splits are used (Irwin et al., 2012). The optimal hyperparameter configuration is chosen by selecting the best average performance over the five validation sets (details in Appendix C.2). One performance metric is reported per dataset. Specifically, predictive accuracy is used for Cora, Citeseer, PubMed, Amazon, Roman Empire, MUTAG, PROTEINS, NCI1, NCI109, IMDB-BIN, IMDB-MUL, and REDDIT; AUC-ROC is used for Minesweeper and Tolokers; mean squared error (MSE) is used for election, bachelor, birth, death, income, migration, and unemployment; and mean absolute error (MAE) is used for ZINC. For each dataset, the mean and standard deviation of the chosen metric are computed across the five test sets and reported in Table 1 (where OOM stands for ‘out of memory’).

5.2 Main Results

As seen from Table 1, higher-order neural networks (based on hypergraphs, simplicial, and cell complexes) achieve the best performance on fifteen of twenty-two datasets, whereas GNNs achieve the best performance on six datasets, and tie on the Unemployment dataset. GNNs perform best on node regression in the majority of cases (five out of seven). These best results obtained by GNNs are closely matched by TNNs, since the latter achieve metrics within one standard deviation from the former. In contrast, in nine out of sixteen datasets

Table 1: Cross-domain comparison: results are shown as mean and standard deviation. The best result is bold and shaded in grey, while those within one standard deviation are in blue-shaded boxes.

	Dataset	GCN	GIN	GAT	AST	EDGNN	UniGNN2	CWN	CCCN	SCCNN	SCN	
Node-level tasks	Cora	87.09 ± 0.20	87.21 ± 1.89	86.71 ± 0.95	88.92 ± 0.44	87.06 ± 1.09	86.97 ± 0.88	86.32 ± 1.38	87.44 ± 1.28	82.19 ± 1.07	82.27 ± 1.34	
	Citeseer	75.53 ± 1.27	73.73 ± 1.23	74.41 ± 1.75	73.85 ± 2.21	74.93 ± 1.39	74.72 ± 1.08	75.20 ± 1.82	75.63 ± 1.58	70.23 ± 2.69	71.24 ± 1.68	
	Pubmed	89.40 ± 0.30	89.29 ± 0.41	89.44 ± 0.24	89.62 ± 0.25	89.04 ± 0.51	89.34 ± 0.45	88.64 ± 0.36	88.52 ± 0.44	88.18 ± 0.32	88.72 ± 0.50	
	Amazon	49.56 ± 0.55	49.16 ± 1.02	50.17 ± 0.59	50.50 ± 0.27	48.18 ± 0.09	49.06 ± 0.08	51.90 ± 0.15	50.26 ± 0.17			OOM
	Empire	78.16 ± 0.32	79.56 ± 0.20	84.02 ± 0.51	79.50 ± 0.13	81.01 ± 0.24	77.06 ± 0.20	81.81 ± 0.62	82.14 ± 0.00	89.15 ± 0.32	88.79 ± 0.46	
	Minesweeper	87.52 ± 0.42	87.82 ± 0.34	89.64 ± 0.43	81.14 ± 0.05	84.52 ± 0.05	78.02 ± 0.00	88.62 ± 0.04	89.42 ± 0.00	89.0 ± 0.00	90.32 ± 0.11	
	Tolokers	83.02 ± 0.71	80.72 ± 1.19	84.43 ± 1.00	83.26 ± 0.10	77.53 ± 0.01	77.35 ± 0.03		OOM	OOM	OOM	OOM
	Election	0.31 ± 0.02	0.28 ± 0.02	0.29 ± 0.02	0.29 ± 0.01	0.34 ± 0.02	0.37 ± 0.02	0.34 ± 0.02	0.31 ± 0.02	0.51 ± 0.03	0.46 ± 0.04	
	Bachelor	0.29 ± 0.02	0.31 ± 0.03	0.28 ± 0.02	0.30 ± 0.03	0.29 ± 0.02	0.31 ± 0.02	0.33 ± 0.03	0.31 ± 0.02	0.34 ± 0.03	0.32 ± 0.02	
	Birth	0.72 ± 0.09	0.72 ± 0.09	0.71 ± 0.09	0.71 ± 0.08	0.70 ± 0.07	0.73 ± 0.10	0.72 ± 0.09	0.71 ± 0.09	0.79 ± 0.12	0.71 ± 0.08	
	Death	0.51 ± 0.04	0.52 ± 0.04	0.51 ± 0.04	0.49 ± 0.05	0.52 ± 0.05	0.51 ± 0.05	0.54 ± 0.06	0.54 ± 0.06	0.55 ± 0.05	0.52 ± 0.05	
	Income	0.22 ± 0.03	0.21 ± 0.02	0.20 ± 0.02	0.21 ± 0.02	0.23 ± 0.02	0.23 ± 0.02	0.25 ± 0.03	0.23 ± 0.02	0.28 ± 0.03	0.25 ± 0.02	
	Migration	0.80 ± 0.12	0.80 ± 0.10	0.77 ± 0.13	0.78 ± 0.12	0.80 ± 0.12	0.79 ± 0.12	0.84 ± 0.13	0.84 ± 0.12	0.90 ± 0.14	0.92 ± 0.20	
	Unempl	0.25 ± 0.03	0.22 ± 0.02	0.23 ± 0.03	0.22 ± 0.02	0.26 ± 0.03	0.28 ± 0.02	0.25 ± 0.03	0.24 ± 0.03	0.43 ± 0.04	0.38 ± 0.04	
	Graph-level tasks	MUTAG	69.79 ± 6.80	79.57 ± 6.13	72.77 ± 2.77	71.06 ± 6.49	80.00 ± 4.90	80.43 ± 4.09	80.43 ± 1.78	77.02 ± 9.32	76.17 ± 6.63	73.62 ± 6.13
PROTEINS		75.70 ± 2.14	75.20 ± 3.30	76.34 ± 1.66	76.63 ± 1.74	73.91 ± 4.39	75.20 ± 2.96	76.13 ± 2.70	73.33 ± 2.30	74.19 ± 2.86	75.27 ± 2.14	
NCII		72.86 ± 0.69	74.26 ± 0.96	75.00 ± 0.99	75.18 ± 1.24	73.97 ± 0.82	73.02 ± 0.92	73.93 ± 1.87	76.67 ± 1.48	76.60 ± 1.75	74.49 ± 1.03	
NCII09		72.20 ± 1.22	74.42 ± 0.70	73.80 ± 0.73	73.75 ± 1.09	74.93 ± 2.50	70.76 ± 1.11	73.80 ± 2.06	75.35 ± 1.50	77.12 ± 1.07	75.70 ± 1.04	
IMDB-BIN		72.00 ± 2.48	70.96 ± 1.93	69.76 ± 2.65	70.32 ± 3.27	69.12 ± 2.92	71.04 ± 1.31	70.40 ± 2.02	69.12 ± 2.82	70.88 ± 2.25	70.80 ± 2.38	
IMDB-MUL		49.97 ± 2.16	47.98 ± 4.21	50.13 ± 3.87	50.51 ± 2.92	49.17 ± 4.35	49.76 ± 3.55	49.71 ± 2.83	47.79 ± 3.45	48.75 ± 3.98	49.49 ± 5.08	
REDDIT		76.24 ± 0.54	81.96 ± 1.36	75.68 ± 1.00	74.84 ± 2.68	83.24 ± 1.45	75.56 ± 3.19	85.52 ± 1.38	85.12 ± 1.29	77.24 ± 1.87	71.28 ± 2.06	
ZINC		0.62 ± 0.01	0.57 ± 0.04	0.61 ± 0.01	0.59 ± 0.02	0.51 ± 0.01	0.60 ± 0.01	0.34 ± 0.01	0.34 ± 0.02	0.36 ± 0.02	0.53 ± 0.04	

TNNs outperform GNNs, and attain performance metrics that are higher by more than one standard deviation with respect to GNNs. In other words, in situations where higher-order networks outperform GNNs, the performance gap is more pronounced. It is also noted that, for demonstration purposes, only one fixed lifting is considered to transform graph data to each of the considered topological domains (see Appendix C.4). These results suggest that, even without lifting optimization, TNNs have an advantage over GNNs in terms of performance, although it is worth emphasizing that overall they also tend to be less efficient in terms of memory usage and computational time than graph-based counterparts (see Appendix C.4 for a more detailed analysis). However, and more importantly for the context of this paper, the benchmarks demonstrate the degree of comparisons that can be performed with TopoBench across models and datasets.

Remark. Notably, OOM results are originated when lifting large, densely connected graphs to higher-order domains, showcasing the scalability issues of the liftings leveraged in this analysis (i.e., clique and cycle liftings to simplicial and cellular domains, respectively).

5.3 Ablation Study

This ablation study examines how different readout strategies influence performance in neural networks built on higher-order domains, highlighting the importance of node-level signal updates and pooling choices. First, graph and hypergraph (neural network) models differ from simplicial and cell complex (neural network) models in terms of the domains and, subsequently, representations they support. Graph and hypergraph models can output two types of representations: node representations and edge or hyperedge representations. In contrast, the output of simplicial and cell models depends on the different types of cells present (0-cell up to n -cells) and on the model itself. For example, a simplicial or cell complex model may process an n -cell input but may not produce an n -cell output. The

`backbone_wrapper` in `TopoBench` addresses these differences in the underlying domains of the models.

There is a second difference, which is inherent in the TNNs themselves. Consider a downstream classification task. For graphs, the standard practice is to perform classification over pooled node features. However, this aspect has not been extensively studied in the TDL literature. For instance, a simplicial or cell model may update 1-cell representations (edges) or 2-cell representations (cycles or triangles) while leaving 0-cell (node) representations unchanged, making direct pooling over nodes potentially ineffective. One could consider more elaborate update processes in which different n -cell representations are combined, but this renders pooling more intricate for higher-order domains. These architectural considerations are complex and remain open research questions in TDL.

Nevertheless, to fairly compare different neural network architectures, this second difference must be addressed. To that end, this ablation study considers two types of readouts to enable a rigorous evaluation: direct readout (DR), where the downstream task is performed directly over the 0-cell representation, and signal down-propagation (SDP), where information from higher-order cell representations is iteratively fused down to 0-cell representations using appropriate incidence matrices, followed by a linear projection over the concatenated $(n - 1)$ -cell signal and the fused $(n - 1)$ -cell representation. For instance, if a simplicial or cell complex model outputs 0-cell, 1-cell, and 2-cell representations, the signal propagates from 2-cells to 1-cells and then from 1-cells to 0-cells during readout. The downstream task is then performed over the updated 0-cell representations.³

Table 2 shows that the best-performing readout type depends on how a model propagates signals internally. For example, the CWN model does not update 0-cell representations, so the SDP strategy performs notably better. Conversely, CCCN, SCCNN, and SCN propagate information to 0-cells, making SDP readout yield only small or negligible changes in performance. Further details are available in Appendix C.4.

These results underscore the impact of structural properties in TNNs. The performance variations observed in this ablation study emphasize the critical role of architectural and lifting decisions for higher-order learning models. By enabling comparisons across a wide range of models and datasets, `TopoBench` facilitates deeper insights and drives advancements in TDL.

5.4 Higher-Order Datasets

Appendix D presents additional illustrative experiments conducted on 13 datasets included in `TopoBench`, spanning a broad range of hypergraph datasets (for classification tasks) and simplicial datasets (for both classification and regression tasks). The evaluation protocol follows the setup described in Section 5.1, with the exception of structural and feature liftings, as these datasets natively possess higher-order topologies and include features on higher-order cells.

For the hypergraph datasets, no single model consistently outperforms others across all benchmarks. Among the evaluated models, `AllSetTransformer` achieves the best performance on 5 out of 10 datasets. For the simplicial MANTRA family of datasets, the results demonstrate that topological tasks are more effectively modeled by TNNs, whereas standard GNN

3. See Appendix A.3 for an introduction to TNNs and Higher-Order Message Passing on topological domains.

Table 2: This ablation study compares the performance of CWN, CCCN, SCCNN, and SCN models on various datasets using two readout strategies, direct readout (DR) and signal down-propagation (SDP). SDP generally enhances CWN performance, whereas the effect of SDP on CCCN, SCCNN, and SCN varies based on their internal signal propagation mechanisms. Means and standard deviations of performance metrics are shown. The best results are shown in bold for each model and readout type.

Dataset	CWN		CCCN		SCCNN		SCN		
	DR	SDP	DR	SDP	DR	SDP	DR	SDP	
Node-level tasks	Cora	74.95 ± 0.98	86.32 ± 1.38	87.44 ± 1.28	87.68 ± 1.17	82.19 ± 1.07	80.65 ± 2.39	82.27 ± 1.34	79.91 ± 1.18
	Citeseer	70.49 ± 2.85	75.20 ± 1.82	75.63 ± 1.58	74.91 ± 1.25	70.23 ± 2.69	69.03 ± 2.01	71.24 ± 1.68	70.40 ± 1.53
	Pubmed	86.94 ± 0.68	88.64 ± 0.36	88.52 ± 0.44	88.67 ± 0.39	88.18 ± 0.32	87.78 ± 0.58	88.72 ± 0.50	88.62 ± 0.44
	Amazon	45.58 ± 0.25	51.90 ± 0.15	50.55 ± 0.15	50.26 ± 0.17	OOM	OOM	OOM	OOM
	Empire	66.13 ± 0.03	81.81 ± 0.62	82.14 ± 0.00	82.51 ± 0.00	89.15 ± 0.32	88.73 ± 0.12	85.89 ± 0.34	88.79 ± 0.46
	Minesweeper	48.82 ± 0.00	88.62 ± 0.04	89.42 ± 0.00	89.85 ± 0.00	87.40 ± 0.00	89.00 ± 0.00	90.32 ± 0.11	90.27 ± 0.36
	Election	0.60 ± 0.04	0.34 ± 0.02	0.31 ± 0.02	0.31 ± 0.01	0.51 ± 0.03	0.56 ± 0.04	0.46 ± 0.04	0.51 ± 0.03
	Bachelor	0.33 ± 0.03	0.33 ± 0.03	0.32 ± 0.02	0.31 ± 0.02	0.34 ± 0.03	0.34 ± 0.03	0.32 ± 0.02	0.32 ± 0.03
	Birth	0.81 ± 0.11	0.72 ± 0.09	0.71 ± 0.09	0.72 ± 0.05	0.79 ± 0.12	0.83 ± 0.12	0.71 ± 0.08	0.80 ± 0.11
	Death	0.55 ± 0.05	0.54 ± 0.06	0.54 ± 0.06	0.54 ± 0.06	0.55 ± 0.05	0.58 ± 0.05	0.52 ± 0.05	0.56 ± 0.05
	Income	0.36 ± 0.04	0.25 ± 0.03	0.23 ± 0.02	0.23 ± 0.02	0.28 ± 0.03	0.31 ± 0.03	0.25 ± 0.02	0.27 ± 0.02
	Migration	0.90 ± 0.16	0.84 ± 0.13	0.84 ± 0.10	0.84 ± 0.12	0.90 ± 0.14	0.93 ± 0.17	0.92 ± 0.20	0.96 ± 0.23
	Unempl	0.46 ± 0.04	0.25 ± 0.03	0.24 ± 0.03	0.25 ± 0.03	0.43 ± 0.04	0.45 ± 0.04	0.38 ± 0.04	0.41 ± 0.03
	Graph-level tasks	MUTAG	69.68 ± 8.58	80.43 ± 1.78	80.85 ± 5.42	77.02 ± 9.32	76.17 ± 6.63	70.64 ± 3.16	71.49 ± 2.43
PROTEINS		76.13 ± 1.80	76.13 ± 2.70	73.55 ± 3.43	73.33 ± 2.30	74.19 ± 2.86	74.98 ± 1.92	75.27 ± 2.14	74.77 ± 1.69
NCI1		68.52 ± 0.51	73.93 ± 1.87	76.67 ± 1.48	77.65 ± 1.28	76.60 ± 1.75	75.60 ± 2.45	75.27 ± 1.57	74.49 ± 1.03
NCI109		68.19 ± 0.65	73.80 ± 2.06	75.35 ± 1.50	74.83 ± 1.18	77.12 ± 1.07	75.43 ± 1.94	74.58 ± 1.29	75.70 ± 1.04
IMDB-BIN		70.40 ± 2.02	69.28 ± 2.57	69.12 ± 2.82	69.44 ± 2.46	70.88 ± 2.25	69.28 ± 5.69	70.80 ± 2.38	68.64 ± 3.90
IMDB-MUL		49.71 ± 2.83	49.87 ± 2.33	49.01 ± 2.63	47.79 ± 3.45	48.75 ± 3.98	46.67 ± 3.13	48.16 ± 2.89	49.49 ± 5.08
REDDIT		76.20 ± 0.86	85.52 ± 1.38	85.12 ± 1.29	83.32 ± 0.73	75.56 ± 3.46	77.24 ± 1.87	71.28 ± 2.06	69.68 ± 4.00
ZINC		0.70 ± 0.00	0.34 ± 0.01	0.35 ± 0.02	0.34 ± 0.02	0.36 ± 0.01	0.36 ± 0.02	0.59 ± 0.01	0.53 ± 0.04

baselines fail to capture the intricate topological structures, resulting in lower performance on purely topological tasks.

6 Concluding Remarks, Limitations, and Future Work

This paper has introduced TopoBench, an open-source benchmarking framework for TDL. By organizing the TDL pipeline into a sequence of modular steps, TopoBench simplifies the benchmarking process and accelerates research. A key feature of TopoBench is its ability to map graph topology and features to higher-order topological domains such as simplicial and cell complexes, enabling richer data representations and more detailed analyses. In addition, TopoBench provides direct access to a wide variety of real and synthetic datasets, covering both graph-based and higher-order domains. The effectiveness of TopoBench has been demonstrated by benchmarking several TDL architectures across diverse learning tasks and datasets, offering insights into the relative advantages of different models.

While TopoBench already addresses several challenges in TDL, it also has limitations that point to promising directions for future enhancements. One area is the implementation of learnable liftings, which are supported by TopoBench. This direction could enable task-specific topological representations learned dynamically from data. A second limitation lies in the broader scarcity of standardized, real-world higher-order datasets. Although TopoBench incorporates numerous datasets for hypergraph, simplicial, and cell complexes,

this remains an active area of expansion. Providing more built-in higher-order datasets will further streamline research in TDL.

Another potential direction is to perform an exhaustive exploration of optimal liftings per combination of domains, datasets, and models. In fact, OOM values showcase the scalability limitations of the most common used strategies to lift graphs into simplicial and cellular domains (i.e., clique and cycle liftings, respectively). Finally, extending the set of evaluation metrics beyond classification or regression accuracy to include more TDL-specific measures of expressivity, explainability, and fairness (Papamarkou et al., 2024) is another avenue of growth—and these modules have been designed to be easily extendable.

Moving forward, the modular design of **TopoBench** invites contributions from the community. Researchers and practitioners are encouraged to contribute to **TopoBench** by introducing new learnable liftings, adding datasets, and developing specialized performance metrics. Moreover, to mitigate the aforementioned scalability issues, several strategies can be explored—e.g. pruning the input graphs prior to lifting, employing scalable lifting mechanisms—such as those explored in the ICML 2024 TDL Challenge (Bernárdez et al., 2024)—and applying mini-batching techniques to higher-order structures in transductive settings (analogous to those used in GNN modeling). These efforts will not only strengthen the benchmarking ecosystem of TDL but also help drive innovation in topological deep learning more broadly—as already shown in the recent works of TopoTune (Papillon et al., 2025) and HOPSE (Carrasco et al., 2025), both of which leverage **TopoBench** framework to push the boundaries of TDL.

Code Availability and Reproducibility

The code for **TopoBench** is publicly available on GitHub under the MIT license: <https://github.com/geometric-intelligence/TopoBench>. The codebase employs continuous integration, is fully documented, and provides comprehensive API documentation at <https://geometric-intelligence.github.io/topobench/index.html>.

All aspects of library installation and development are described in the `README.md` file. To replicate the experiments reported in this paper, refer to the ‘Experiments Reproducibility’ section in `README.md`. Additional tutorials in the ‘Tutorials’ section illustrate how to integrate new models, datasets, learnable liftings, and transforms within **TopoBench**.

Broader Impact Statement

TopoBench aims to standardize benchmarking in TDL, thus benefiting the community by facilitating and accelerating research developments in TDL and its applications. We do not expect **TopoBench** to have any direct negative societal impact from its usage. Moreover, the code of conduct for **TopoBench** contributors, which is publicly available in the ‘`README.md`’ file of the GitHub repository of the library, sets concrete ethical standards, promotes transparency, fairness, and inclusivity in research.

The **TopoBench** library will be constantly maintained to respect proprietary content. It will implement strict revision processes to ensure that all code implementations, libraries, and datasets have open-source licenses that guarantee their legitimate usage within the framework.

Author Contributions

L. Telyatnikov and G. Bernárdez contributed equally to this work as the main authors and lead developers. The conceptualization of the TopoBench project was a collaborative effort by L. Telyatnikov, G. Bernárdez, M. Montagna, N. Miolane, T. Papamarkou, M. Hajij, G. Zamzmi, M. T. Schaub, and S. Scardapane. The core development and implementation of the benchmark were carried out by L. Telyatnikov, G. Bernárdez, M. Montagna, M. Carrasco, P. Vasylenko, M. Papillon, and N. Miolane. The experiments were led by L. Telyatnikov with support from G. Bernárdez. The manuscript was written by T. Papamarkou, L. Telyatnikov, and G. Bernárdez, with significant writing contributions to various sections from S. Scardapane, M. Hajij, G. Zamzmi, and M. T. Schaub. All other authors contributed to the TopoBench ecosystem through their winning submissions (i.e. lifting implementations) to the ICML TDL Challenge 2024 (Bernárdez et al., 2024).

Acknowledgments and Disclosure of Funding

M. Papillon, G. Bernárdez and N. Miolane acknowledge support from the National Science Foundation, Award DMS-2134241. M. Papillon and N. Miolane acknowledge funding from the National Science Foundation, Award DMS-2240158 and from the Noyce Foundation. M. Papillon acknowledges the support of the Natural Sciences and Engineering Research Council of Canada. M. Hajij acknowledges support from the National Science Foundation, award DMS-2134231. M. T. Schaub acknowledges funding by the European Union (ERC, HIGH-HOPeS, 101039827). Views and opinions expressed are however those of the author(s) only and do not necessarily reflect those of the European Union or the European Research Council Executive Agency. Neither the European Union nor the granting authority can be held responsible for them.

References

- Rubén Ballester, Ernst Röell, Daniel Bin Schmid, Mathieu Alain, Sergio Escalera, Carles Casacuberta, and Bastian Rieck. Mantra: The manifold triangulations assemblage. *arXiv preprint arXiv:2410.02392*, 2024.
- Sergio Barbarossa and Stefania Sardellitti. Topological signal processing over simplicial complexes. *IEEE Transactions on Signal Processing*, 68:2992–3007, 2020.
- Claudio Battiloro, Indro Spinelli, Lev Telyatnikov, Michael M. Bronstein, Simone Scardapane, and Paolo Di Lorenzo. From latent graph to latent topology inference: Differentiable cell complex module. In *The Twelfth International Conference on Learning Representations*, 2024a. URL <https://openreview.net/forum?id=0JsRZEGZ7L>.
- Claudio Battiloro, Lucia Testa, Lorenzo Giusti, Stefania Sardellitti, Paolo Di Lorenzo, and Sergio Barbarossa. Generalized simplicial attention neural networks. *IEEE Transactions on Signal and Information Processing over Networks*, 10:833–850, 2024b. doi: 10.1109/TSIPN.2024.3485473.

- Claudio Battiloro, Ege Karaismailoglu, Mauricio Tec, George Dasoulas, Michelle Audirac, and Francesca Dominici. E(n) equivariant topological neural networks. In *The Thirteenth International Conference on Learning Representations*, 2025. URL <https://openreview.net/forum?id=Ax3uliEBVR>.
- Federico Battiston, Enrico Amico, Alain Barrat, Ginestra Bianconi, Guilherme Ferraz de Arruda, Benedetta Franceschiello, Iacopo Iacopini, Sonia Kéfi, Vito Latora, Yamir Moreno, et al. The physics of higher-order interactions in complex systems. *Nature Physics*, 17(10): 1093–1098, 2021.
- Guillermo Bernárdez, Lev Telyatnikov, Eduard Alarcón, Albert Cabellos-Aparicio, Pere Barlet-Ros, and Pietro Liò. Topological network traffic compression. In *Proceedings of the 2nd on Graph Neural Networking Workshop 2023*, pages 7–12, 2023.
- Guillermo Bernárdez, Lev Telyatnikov, Marco Montagna, Federica Baccini, Mathilde Papillon, Miquel Ferriol-Galmés, Mustafa Hajij, Theodore Papamarkou, Maria Sofia Bucarelli, Olga Zaghen, et al. Icml topological deep learning challenge 2024: Beyond the graph domain. *arXiv preprint arXiv:2409.05211*, 2024.
- Guillermo Bernárdez, Miquel Ferriol-Galmés, Carlos Güemes-Palau, Mathilde Papillon, Pere Barlet-Ros, Albert Cabellos-Aparicio, and Nina Miolane. Ordered topological deep learning: a network modeling case study, 2025. URL <https://arxiv.org/abs/2503.16746>.
- Christian Bick, Elizabeth Gross, Heather A Harrington, and Michael T Schaub. What are higher-order networks? *SIAM Review*, 65(3):686–731, 2023.
- Cristian Bodnar. *Topological deep learning: graphs, complexes, sheaves*. PhD thesis, University of Cambridge, 2023.
- Cristian Bodnar, Fabrizio Frasca, Nina Otter, Yuguang Wang, Pietro Lio, Guido F Montufar, and Michael Bronstein. Weisfeiler and Lehman go cellular: CW networks. *Advances in Neural Information Processing Systems*, 2021a.
- Cristian Bodnar, Fabrizio Frasca, Yuguang Wang, Nina Otter, Guido F Montufar, Pietro Lio, and Michael Bronstein. Weisfeiler and Lehman go topological: Message passing simplicial networks. In *International Conference on Machine Learning*, 2021b.
- Michael M Bronstein, Joan Bruna, Taco Cohen, and Petar Veličković. Geometric deep learning: Grids, groups, graphs, geodesics, and gauges. *arXiv preprint arXiv:2104.13478*, 2021.
- Eric Bunch, Qian You, Glenn Fung, and Vikas Singh. Simplicial 2-complex convolutional neural nets. In *NeurIPS Workshop on Topological Data Analysis and Beyond*, 2020.
- Martin Carrasco, Guillermo Bernardez, Marco Montagna, Nina Miolane, and Lev Telyatnikov. Hopse: Scalable higher-order positional and structural encoder for combinatorial representations. *arXiv preprint arXiv:2505.15405*, 2025.

- Ding-Yun Chen, Xiao-Pei Tian, Yu-Te Shen, and Ming Ouhyoung. On visual similarity based 3d model retrieval. In *Computer graphics forum*, volume 22, pages 223–232. Wiley Online Library, 2003.
- Yuzhou Chen, Yulia R Gel, and H Vincent Poor. BScNets: block simplicial complex neural networks. In *Proceedings of the AAAI Conference on Artificial Intelligence*, 2022.
- Eli Chien, Chao Pan, Jianhao Peng, and Olgica Milenkovic. You are allset: a multiset function framework for hypergraph neural networks. *arXiv preprint arXiv:2106.13264*, 2021.
- Yihe Dong, Will Sawin, and Yoshua Bengio. HNHN: hypergraph networks with hyperedge neurons. In *ICML Graph Representation Learning and Beyond Workshop*, 2020.
- Dheeru Dua, Casey Graff, et al. Uci machine learning repository, 2017. URL <http://archive.ics.uci.edu/ml>, 7(1), 2017.
- Vijay Prakash Dwivedi, Chaitanya K Joshi, Anh Tuan Luu, Thomas Laurent, Yoshua Bengio, and Xavier Bresson. Benchmarking graph neural networks. *Journal of Machine Learning Research*, 24(43):1–48, 2023.
- Stefania Ebli, Michaël Defferrard, and Gard Spreemann. Simplicial neural networks. In *NeurIPS Workshop on Topological Data Analysis and Beyond*, 2020.
- Yifan Feng, Haoxuan You, Zizhao Zhang, Rongrong Ji, and Yue Gao. Hypergraph neural networks. In *Proceedings of the AAAI Conference on Artificial Intelligence*, 2019.
- Matthias Fey and Jan E. Lenssen. Fast graph representation learning with PyTorch Geometric. In *ICLR Workshop on Representation Learning on Graphs and Manifolds*, 2019.
- Lorenzo Giusti, Claudio Battiloro, Paolo Di Lorenzo, Stefania Sardellitti, and Sergio Barbarossa. Simplicial attention neural networks. *arXiv preprint arXiv:2203.07485*, 2022.
- Lorenzo Giusti, Claudio Battiloro, Lucia Testa, Paolo Di Lorenzo, Stefania Sardellitti, and Sergio Barbarossa. Cell attention networks. In *International Joint Conference on Neural Networks*, 2023.
- Rafael Gómez-Bombarelli, Jennifer N Wei, David Duvenaud, José Miguel Hernández-Lobato, Benjamín Sánchez-Lengeling, Dennis Sheberla, Jorge Aguilera-Iparraguirre, Timothy D Hirzel, Ryan P Adams, and Alán Aspuru-Guzik. Automatic chemical design using a data-driven continuous representation of molecules. *ACS central science*, 4(2):268–276, 2018.
- Aric Hagberg, Pieter Swart, and Daniel S Chult. Exploring network structure, dynamics, and function using NetworkX. Technical report, Los Alamos National Lab (LANL), Los Alamos, NM, United States, 2008.
- Mustafa Hajij, Kyle Istvan, and Ghada Zamzmi. Cell complex neural networks. In *NeurIPS Workshop on Topological Data Analysis and Beyond*, 2020.

- Mustafa Hajij, Ghada Zamzmi, Theodore Papamarkou, Aldo Guzman-Saenz, Tolga Birdal, and Michael T Schaub. Combinatorial complexes: bridging the gap between cell complexes and hypergraphs. In *2023 57th Asilomar Conference on Signals, Systems, and Computers*, pages 799–803. IEEE, 2023a.
- Mustafa Hajij, Ghada Zamzmi, Theodore Papamarkou, Nina Miolane, Aldo Guzmán-Sáenz, Karthikeyan Natesan Ramamurthy, Tolga Birdal, Tamal Dey, Soham Mukherjee, Shreyas Samaga, Neal Livesay, Robin Walters, Paul Rosen, and Michael Schaub. Topological deep learning: going beyond graph data. *arXiv preprint arXiv:1906.09068*, 2023b.
- Mustafa Hajij, Mathilde Papillon, Florian Frantzen, Jens Agerberg, Ibrahim AlJabea, Rubén Ballester, Claudio Battiloro, Guillermo Bernárdez, Tolga Birdal, Aiden Brent, Peter Chin, Sergio Escalera, Simone Fiorellino, Odin Hoff Gardaa, Gurusankar Gopalakrishnan, Devendra Govil, Josef Hoppe, Maneel Reddy Karri, Jude Khouja, Manuel Lecha, Neal Livesay, Jan Meißner, Soham Mukherjee, Alexander Nikitin, Theodore Papamarkou, Jaro Prilepok, Karthikeyan Natesan Ramamurthy, Paul Rosen, Aldo Guzmán-Sáenz, Alessandro Salatiello, Shreyas N. Samaga, Simone Scardapane, Michael T. Schaub, Luca Scofano, Indro Spinelli, Lev Telyatnikov, Quang Truong, Robin Walters, Maosheng Yang, Olga Zaghien, Ghada Zamzmi, Ali Zia, and Nina Miolane. TopoX: a suite of Python packages for machine learning on topological domains. *Journal of Machine Learning Research*, 25 (374):1–8, 2024.
- Weihua Hu, Matthias Fey, Marinka Zitnik, Yuxiao Dong, Hongyu Ren, Bowen Liu, Michele Catasta, and Jure Leskovec. Open graph benchmark: datasets for machine learning on graphs. In *Advances in Neural Information Processing Systems*, pages 22118–22133, 2020.
- Weihua Hu, Matthias Fey, Hongyu Ren, Maho Nakata, Yuxiao Dong, and Jure Leskovec. OGB-LSC: a large-scale challenge for machine learning on graphs. *arXiv preprint arXiv:2103.09430*, 2021.
- Jing Huang and Jie Yang. UniGNN: a unified framework for graph and hypergraph neural networks. In *Proceedings of the Thirtieth International Joint Conference on Artificial Intelligence*, 2021.
- John J Irwin, Teague Sterling, Michael M Mysinger, Erin S Bolstad, and Ryan G Coleman. ZINC: a free tool to discover chemistry for biology. *Journal of Chemical Information and Modeling*, 52(7):1757–1768, 2012.
- Kanchan Jha, Sriparna Saha, and Hiteshi Singh. Prediction of protein–protein interaction using graph neural networks. *Scientific Reports*, 12(1):1–12, 2022.
- Junteng Jia and Austion R Benson. Residual correlation in graph neural network regression. In *ACM International Conference on Knowledge Discovery and Data Mining*, 2020.
- Anees Kazi, Luca Cosmo, Seyed-Ahmad Ahmadi, Nassir Navab, and Michael M Bronstein. Differentiable graph module (dgm) for graph convolutional networks. *IEEE Transactions on Pattern Analysis and Machine Intelligence*, 45(2):1606–1617, 2022.

- Thomas N Kipf and Max Welling. Semi-supervised classification with graph convolutional networks. *arXiv preprint arXiv:1609.02907*, 2016.
- David Knoke and Song Yang. *Social network analysis*. SAGE Publications, 2019.
- Nicholas W. Landry, Maxime Lucas, Iacopo Iacopini, Giovanni Petri, Alice Schwarze, Alice Patania, and Leo Torres. XGI: a Python package for higher-order interaction networks. *Journal of Open Source Software*, 8(85):5162, 2023.
- Mona Lisa and Hew Bot. My Research Software, 12 2017. URL <https://github.com/github-linguist/linguist>.
- Xu T Liu, Jesun Firoz, Andrew Lumsdaine, Cliff Joslyn, Sinan Aksoy, Brenda Praggastis, and Assefaw H Gebremedhin. Parallel algorithms for efficient computation of high-order line graphs of hypergraphs. In *International Conference on High Performance Computing, Data, and Analytics*, 2021.
- Christopher Morris, Nils M. Kriege, Franka Bause, Kristian Kersting, Petra Mutzel, and Marion Neumann. TUDataset: a collection of benchmark datasets for learning with graphs. In *ICML Workshop on Graph Representation Learning and Beyond*, 2020.
- Chris Tralie Nathaniel Saul. Scikit-tda: Topological data analysis for python, 2019. URL <https://doi.org/10.5281/zenodo.2533369>.
- Theodore Papamarkou, Tolga Birdal, Michael M. Bronstein, Gunnar E. Carlsson, Justin Curry, Yue Gao, Mustafa Hajij, Roland Kwitt, Pietro Lio, Paolo Di Lorenzo, Vasileios Maroulas, Nina Miolane, Farzana Nasrin, Karthikeyan Natesan Ramamurthy, Bastian Rieck, Simone Scardapane, Michael T Schaub, Petar Veličković, Bei Wang, Yusu Wang, Guowei Wei, and Ghada Zamzmi. Position: Topological deep learning is the new frontier for relational learning. In *Proceedings of the 41st International Conference on Machine Learning*, volume 235 of *Proceedings of Machine Learning Research*, pages 39529–39555, 2024.
- Mathilde Papillon, Sophia Sanborn, Mustafa Hajij, and Nina Miolane. Architectures of topological deep learning: a survey on topological neural networks. *arXiv preprint arXiv:2304.10031*, 2023.
- Mathilde Papillon, Guillermo Bernárdez, Claudio Battiloro, and Nina Miolane. Topotune : A framework for generalized combinatorial complex neural networks. In *Forty-second International Conference on Machine Learning*, 2025. URL <https://openreview.net/pdf?id=S5njonQdBf>.
- Oleg Platonov, Denis Kuznedelev, Michael Diskin, Artem Babenko, and Liudmila Prokhorenkova. A critical look at the evaluation of GNNs under heterophily: are we really making progress? *arXiv preprint arXiv:2302.11640*, 2023.
- Karthikeyan Natesan Ramamurthy, Aldo Guzmán-Sáenz, and Mustafa Hajij. Topo-MLP: a simplicial network without message passing. In *International Conference on Acoustics, Speech and Signal Processing*, 2023.

- T. Mitchell Roddenberry, Nicholas Glaze, and Santiago Segarra. Principled simplicial neural networks for trajectory prediction. In *International Conference on Machine Learning*, 2021.
- Benedek Rozemberczki, Oliver Kiss, and Rik Sarkar. Karate Club: an API oriented open-source Python framework for unsupervised learning on graphs. In *ACM International Conference on Information and Knowledge Management*, 2020.
- Benjamin Sanchez-Lengeling, Emily Reif, Adam Pearce, and Alexander B. Wiltschko. A gentle introduction to graph neural networks. *Distill*, 6(9):e33, 2021.
- Michael T. Schaub, Yu Zhu, Jean-Baptiste Seby, T. Mitchell Roddenberry, and Santiago Segarra. Signal processing on higher-order networks: livin’ on the edge... and beyond. *Signal Processing*, 187:108149, 2021.
- Hang Su, Subhransu Maji, Evangelos Kalogerakis, and Erik Learned-Miller. Multi-view convolutional neural networks for 3d shape recognition. In *Proceedings of the IEEE international conference on computer vision*, pages 945–953, 2015.
- Guillaume Tautzin, Umberto Lupo, Lewis Tunstall, Julian Burella Pérez, Matteo Caorsi, Anibal M Medina-Mardones, Alberto Dassatti, and Kathryn Hess. giotto-tda: A topological data analysis toolkit for machine learning and data exploration. *Journal of Machine Learning Research*, 22(39):1–6, 2021.
- Lev Telyatnikov and Simone Scardapane. Egg-gae: scalable graph neural networks for tabular data imputation. In Francisco Ruiz, Jennifer Dy, and Jan-Willem van de Meent, editors, *Proceedings of The 26th International Conference on Artificial Intelligence and Statistics*, volume 206 of *Proceedings of Machine Learning Research*, pages 2661–2676. PMLR, 25–27 Apr 2023. URL <https://proceedings.mlr.press/v206/telyatnikov23a.html>.
- Lev Telyatnikov, Maria Sofia Bucarelli, Guillermo Bernardez, Olga Zaghen, Simone Scardapane, and Pietro Lio. Hypergraph neural networks through the lens of message passing: A common perspective to homophily and architecture design. *Transactions on Machine Learning Research*, 2025. ISSN 2835-8856. URL <https://openreview.net/forum?id=8rxtL0kZnX>.
- The GUDHI Project. *GUDHI User and Reference Manual*. GUDHI Editorial Board, 2015. URL <http://gudhi.gforge.inria.fr/doc/latest/>.
- Petar Veličković, Guillem Cucurull, Arantxa Casanova, Adriana Romero, Pietro Lio, and Yoshua Bengio. Graph attention networks. In *International Conference on Learning Representations*, 2018.
- Minjie Wang, Da Zheng, Zihao Ye, Quan Gan, Mufei Li, Xiang Song, Jinjing Zhou, Chao Ma, Lingfan Yu, Yu Gai, Tianjun Xiao, Tong He, George Karypis, Jinyang Li, and Zheng Zhang. Deep Graph Library: a graph-centric, highly-performant package for graph neural networks. *arXiv preprint arXiv:1909.01315*, 2019.
- Peihao Wang, Shenghao Yang, Yunyu Liu, Zhangyang Wang, and Pan Li. Equivariant hypergraph diffusion neural operators. *arXiv preprint arXiv:2207.06680*, 2022.

- Peihao Wang, Shenghao Yang, Yunyu Liu, Zhangyang Wang, and Pan Li. Equivariant hypergraph diffusion neural operators. In *The Eleventh International Conference on Learning Representations*, 2023. URL <https://openreview.net/forum?id=RiTjKoscnNd>.
- Amaury Wei and Olga Fink. Physics meets topology: Physics-informed topological neural networks for learning rigid body dynamics. *arXiv preprint arXiv:2411.11467*, 2024.
- Zhirong Wu, Shuran Song, Aditya Khosla, Fisher Yu, Linguang Zhang, Xiaoou Tang, and Jianxiong Xiao. 3d shapenets: A deep representation for volumetric shapes. In *Proceedings of the IEEE conference on computer vision and pattern recognition*, pages 1912–1920, 2015.
- Keyulu Xu, Weihua Hu, Jure Leskovec, and Stefanie Jegelka. How powerful are graph neural networks? In *International Conference on Learning Representations*, 2019.
- Omry Yadan. Hydra - a framework for elegantly configuring complex applications. Github, 2019. URL <https://github.com/facebookresearch/hydra>.
- Naganand Yadati, Madhav Nimishakavi, Prateek Yadav, Vikram Nitin, Anand Louis, and Partha Talukdar. Hypergen: A new method for training graph convolutional networks on hypergraphs. *Advances in neural information processing systems*, 32, 2019.
- Chaoqi Yang, Ruijie Wang, Shuochao Yao, and Tarek Abdelzaher. Hypergraph learning with line expansion. *arXiv preprint arXiv:2005.04843*, 2020.
- Maosheng Yang and Elvin Isufi. Convolutional learning on simplicial complexes. *arXiv preprint arXiv:2301.11163*, 2023.
- Ruochen Yang, Frederic Sala, and Paul Bogdan. Efficient representation learning for higher-order data with simplicial complexes. In *Learning on Graphs Conference*, 2022.
- Zhilin Yang, William Cohen, and Ruslan Salakhudinov. Revisiting semi-supervised learning with graph embeddings. In *International conference on machine learning*, pages 40–48. PMLR, 2016.
- Jie Zhou, Guanghui Cui, Shengding Hu, Zhengyan Zhang, Cheng Yang, Zhiyuan Liu, and Maosong Sun. Graph neural networks: A review of methods and applications. *AI Open*, 1: 57–81, 2020.

Appendix A. Mathematical Background

Relational data modeling is a fundamental aspect of modern machine learning and data analysis, particularly in domains where complex relationships between entities play a crucial role. This appendix provides a comprehensive overview of the key concepts and techniques in relational data modeling, with a focus on topological approaches that capture intricate structural information. It also provides the essential mathematical background required to effectively use `TopoBench`.

We begin by exploring various topological domains, from the familiar terrain of graphs to more sophisticated structures such as hypergraphs, simplicial complexes, cell complexes,

and combinatorial complexes (see Appendix A.1). These domains offer powerful frameworks for representing and analyzing complex relational data⁴. Next, we introduce the *lifting mechanism*, which enables the mapping of one topological domain onto another, facilitating flexible data representations (refer to Appendix A.2). Finally, we conclude by presenting a mathematical introduction to Topological Neural Networks, which are used to model data represented with the help of one of the topological domains (see Appendix A.3).

A.1 Topological Domains

This section introduces the topological domains implemented in **TopoBench**, which provide powerful frameworks for modeling complex relationships and structures in data. We begin with the fundamental concept of graphs, laying the groundwork for understanding more intricate structures. From there, we explore higher-order domains — including hypergraphs, simplicial complexes, cell complexes, and combinatorial complexes — each offering unique capabilities for capturing different types of relationships and hierarchies within data.

Definition 1 *Let $\mathcal{G} = (V, E)$ be a graph, with node set V and edge set E . A featured graph is a tuple $\mathcal{G}_F = (V, E, F_V, F_E)$, where $F_V : V \rightarrow \mathbb{R}^{d_v}$ is a function that maps each node to a feature vector in \mathbb{R}^{d_v} and $F_E : E \rightarrow \mathbb{R}^{d_e}$ is a function that maps each edge to a feature vector in \mathbb{R}^{d_e} .*

A topological domain is a generalization of a graph that captures both pairwise and higher-order relationships between entities (Bick et al., 2023; Battiston et al., 2021). When working with topological domains, two key properties come into play: set-type relations and hierarchical structures represented by rank functions (Hajij et al., 2023b; Papillon et al., 2023).

Definition 2 (Set-type relation) *A relation in a topological domain is called a set-type relation if its existence is not implied by another relation in the domain.*

Definition 3 (Rank function) *A rank function on a higher-order domain \mathcal{X} is an order-preserving function $rk : \mathcal{X} \rightarrow \mathbb{Z}_{\geq 0}$ such that $x \subseteq y$ implies $rk(x) \leq rk(y)$ for all $x, y \in \mathcal{X}$.*

Set-type relations emphasize the independence of connections within a domain, allowing for flexible representation of complex interactions. In contrast, rank functions introduce a hierarchical (also referred to as part-whole) organization that facilitates the representation and analysis of nested relationships.

Hypergraphs Hypergraphs generalize traditional graphs by allowing edges, known as hyperedges, to connect any number of nodes. This flexibility enables hypergraphs to capture more complex relationships between entities than standard graphs, which only connect pairs of nodes. Hypergraphs exhibit set-type relationships that lack an explicit notion of hierarchy. Using these set-type relations makes them a powerful tool for representing relationships across a diverse range of complex systems.

4. **TopoBench** supports simplicial complexes, cell complexes, hypergraphs, and combinatorial complexes. The **TopoBench** modularity allows for easy addition of other topological domains.

Definition 4 (Hypergraph) *A hypergraph \mathcal{H} on a nonempty set \mathcal{V} is a pair $(\mathcal{V}, \mathcal{E}_{\mathcal{H}})$, where $\mathcal{E}_{\mathcal{H}}$ is a non-empty subset of the powerset $\mathcal{P}(\mathcal{V}) \setminus \{\emptyset\}$. Elements of $\mathcal{E}_{\mathcal{H}}$ are called hyperedges.*

Example 1 (Collaborative Authorship Networks) *In collaborative networks, authors are represented as nodes, and co-authorship on a paper forms a hyperedge connecting all authors involved.*

Simplicial complexes Simplicial complexes extend graphs by incorporating hierarchical part-whole relationships through the multi-scale construction of cells. In this structure, nodes correspond to rank 0-cells, which can be combined to form edges (rank 1-cells). Edges can then be grouped to form faces (rank 2 cells), and faces can be combined to create volumes (rank 3-cells), continuing in this manner. Consequently, the faces of a simplicial complex are triangles, volumes are tetrahedrons, and higher-dimensional cells follow the same pattern. A key feature of simplicial complexes is their strict hierarchical structure, where each k -dimensional simplex is composed of $(k - 1)$ -dimensional simplices, reinforcing a strong sense of hierarchy across all levels.

Definition 5 (Simplicial Complex) *A simplicial complex (SC) in a non-empty set S is a pair $SC = (S, \mathcal{X})$, where $\mathcal{X} \subset \mathcal{P}(S) \setminus \{\emptyset\}$ satisfies: if $x \in SC$ and $y \subseteq x$, then $y \in SC$. The elements of \mathcal{X} are called simplices.*

Example 2 (3D Surface Meshes) *3D models of objects, such as those used in computer graphics or for representing anatomical structures, are often constructed using triangular meshes. These meshes naturally form simplicial complexes, where the vertices of the triangles are 0-simplices, the edges are 1-simplices, and the triangular faces themselves are 2-simplices.*

Cell complexes Cell complexes provide a hierarchical interior-to-boundary structure, offering clear topological and geometric interpretations, but they are not based on set-type relations. Unlike simplicial complexes, cell complexes are not limited to simplices; faces can involve more than three nodes, allowing for a more flexible representation. This increased flexibility grants cell complexes greater expressivity compared to simplicial complexes Bodnar et al. (2021a); Bodnar (2023).

Definition 6 (Cell complex) *A regular cell complex is a topological space S partitioned into subspaces (cells) $\{x_{\alpha}\}_{\alpha \in P_S}$, where P_S is an index set, satisfying:*

1. $S = \cup_{\alpha \in P_S} \text{int}(x_{\alpha})$, where $\text{int}(x)$ denotes the interior of cell x .
2. For each $\alpha \in P_S$, there exists a homeomorphism ψ_{α} (attaching map) from x_{α} to $\mathbb{R}^{n_{\alpha}}$ for some $n_{\alpha} \in \mathbb{N}$. The integer n_{α} is the dimension of cell x_{α} .
3. For each cell x_{α} , the boundary ∂x_{α} is a union of finitely many cells of strictly lower dimension.

Example 3 (Molecular structures.) *Molecules admit natural representations as cell complexes by considering atoms as nodes (i.e., cells of rank zero), bonds as edges (i.e., cells of rank one), and rings as faces (i.e., cells of rank two).*

Combinatorial complexes Combinatorial complexes combine hierarchical structure with set-type relations, enabling a flexible yet comprehensive representation of higher-order networks.

Definition 7 (Combinatorial complex) *A combinatorial complex (CC) is a triple $(\mathcal{V}, \mathcal{X}, \text{rk})$ consisting of a set \mathcal{V} , a subset $\mathcal{X} \subset \mathcal{P}(\mathcal{V}) \setminus \{\emptyset\}$, and a function $\text{rk}: \mathcal{X} \rightarrow \mathbb{Z}_{\geq 0}$ satisfying:*

1. For all $v \in \mathcal{V}$, $\{v\} \in \mathcal{X}$ and $\text{rk}(v) = 0$.
2. The function rk is order-preserving: if $x, y \in \mathcal{X}$ with $x \subseteq y$, then $\text{rk}(x) \leq \text{rk}(y)$.

Example 4 (Geospatial structures.) *Geospatial data, comprised of grid points (0-cells), road polylines (1-cells), and census tract polygons (2-cells), can be effectively represented using combinatorial complexes. A visual example is provided in Figure 2 (Right) of Battiloro et al. (2025).*

Featured topological domains. A featured graph is a graph whose nodes or edges are equipped with feature functions (Sanchez-Lengeling et al., 2021). **TopoBench** generalizes this idea to featured topological domains, where each topological element (e.g., simplex or cell) can carry feature vectors. Although the following definitions use cell complexes as a template, the same ideas apply to other domains (simplicial complexes, hypergraphs, and so on).

Definition 8 (Featured topological domain) *A featured topological domain is a pair (\mathcal{X}, F) , where \mathcal{X} is a topological domain and $F = \{F_i\}_{i \geq 0}$ is a collection of feature functions. Each function F_i maps the i -dimensional elements of \mathcal{X} , denoted \mathcal{X}_i , to a feature space \mathbb{R}^{k_i} :*

$$F_i: \mathcal{X}_i \rightarrow \mathbb{R}^{k_i}.$$

A.2 Liftings

Lifting describes the process of mapping two topological domains through a well-defined procedure (Hajij et al., 2023b; Papillon et al., 2023). This work extends this concept by providing a unified mathematical framework that generalizes all lifting procedures from the 2nd Topological Deep Learning Challenge at ICML 2024 (Bernárdez et al., 2024).

Definition 9 (Lifting between featured topological domains) *Let $T_1 = (\mathcal{X}_1, F_1)$ and $T_2 = (\mathcal{X}_2, F_2)$ be two featured topological domains. A lifting from T_1 to T_2 is a pair (ψ_X, ψ_F) , where:*

1. **Structural lifting** $\psi_X: \mathcal{X}_1 \times F_1 \rightarrow \mathcal{X}_2$ is a map that determines how elements of \mathcal{X}_1 are mapped into \mathcal{X}_2 .
2. **Feature lifting** $\psi_F: \mathcal{X}_1 \times F_1 \rightarrow F_2$ is a map that transforms feature functions while maintaining consistency with ψ_X , meaning that for all $x \in \mathcal{X}_1$,

$$F_2(\psi_X(x)) = \psi_F(F_1(x)).$$

In practice, structural liftings can be taxonimized as *connectivity-* and/or *feature-based*. Connectivity-based structural lifting ψ_X maps the elements of \mathcal{X}_1 to \mathcal{X}_2 relying solely on the given topology \mathcal{X}_1 . In contrast, feature-based structural lifting leverages the features F_1 either to conditionally guide the mapping of topology or to fully infer the topology \mathcal{X}_2 from F_1 . The feature lifting ψ_F further ensures that the associated features are consistently transferred. Examples appear in Figure 3.

A.2.1 LIFTING EXAMPLES

In this section, we present four examples of lifting from the graph domain to higher-order topological domains (see Examples 5, 6, 7, and 8), followed by two application examples demonstrating how topological domains can be used to describe real-world data (see Examples 9 and 10).

Example 5 *From graphs to cell complexes: cycle-based liftings.* *A graph is lifted to a cell complex in two steps. First, a finite set of cycles (closed loops) within the graph is identified. Second, each identified cycle is associated with a 2-cell whose boundary is exactly that cycle. The nodes and edges of the cell complex are inherited from the original graph.*

Example 6 *From graphs to simplicial complexes: clique complexes.* *By lifting a graph to a simplicial complex, both pairwise and higher-order interactions can be captured. For a given graph, the corresponding clique complex is formed by treating every complete subgraph (clique) as a simplex. Specifically, each node is a 0-simplex, each edge (clique of size 2) is a 1-simplex, each triangle (clique of size 3) is a 2-simplex, and so forth. In general, a clique of size $k + 1$ becomes a k -simplex.*

Example 7 *From graphs to simplicial complexes: neighbor complexes.* *Neighbor complexes lift the neighborhoods of nodes to simplices as follows. For each node in the graph, the node itself and all its neighbors are considered as a single set. This set is then treated as a simplex, whose dimension depends on the node’s degree. For instance, if a node has d neighbors, it forms a d -simplex.*

Example 8 *From graphs to hypergraphs: k-hop liftings.* *Let $\mathcal{G} = (V, E)$ be a graph and $\mathcal{H} = (V, \mathcal{E})$ be a hypergraph. The k -neighborhood $N_k(v)$ of a node $v \in V$ in \mathcal{G} consists of all nodes reachable within k steps from v . To lift \mathcal{G} to \mathcal{H} , a hyperedge e_v is assigned to each node $v \in V$ in \mathcal{H} , where $e_v = N_k(v)$. Thus, the set of hyperedges in \mathcal{H} is given by $\mathcal{E} = \{N_k(v) \mid v \in V\}$.*

Example 9 *Lifting a Social Network to a Higher-Order Topological Domain.* *Let T_1 be a social network represented as a graph, where nodes correspond to individuals and edges indicate social interactions (e.g., friendships, collaborations, or message exchanges). We lift this structure to a hypergraph or simplicial complex T_2 , where higher-order interactions capture group dynamics beyond pairwise relationships.*

- *The structural lifting ψ_X maps tightly connected communities or recurring social interactions in T_1 to higher-order simplices in T_2 . For instance, a group of researchers collaborating on multiple papers could be lifted from a clique in T_1 to a 3-simplex in T_2 , representing a collective research effort.*

- The feature lifting ψ_F aggregates individual attributes (e.g., influence score, topic preferences, engagement level) into group-level properties (e.g., collective expertise, community sentiment, or information diffusion capacity).

Example 10 *Lifting Molecular Simplicial Complexes to Cell Complexes.* Consider T_1 as a simplicial complex derived from a molecular structure, where nodes represent atoms, edges represent bonds, and 2-simplices represent stable chemical rings. Suppose we lift this structure to a cell complex T_2 that includes larger functional groups such as benzene rings or protein substructures.

- The structural lifting ψ_X embeds lower-dimensional simplices into a coarser representation of molecular geometry, grouping functionally related simplices into higher-dimensional cells.
- The feature lifting ψ_F ensures that atomic properties (e.g., electronegativity, charge distribution) are mapped to molecular functional groups, enabling efficient coarse-grained learning in topological graph neural networks.

Lifting maps can be either *fixed* (Bodnar et al., 2021a; Hajij et al., 2023b) or *learnable* (Battiloro et al., 2024a; Bernárdez et al., 2023; Telyatnikov and Scardapane, 2023; Ramamurthy et al., 2023; Kazi et al., 2022), and they may compute or learn both the features on higher-order cells and the structure of the domain itself.

A.3 Topological Neural Networks

A.3.1 GENERAL DEFINITION

Topological neural networks (TNNs) are neural architectures that process data defined on topological domains. The higher-order message passing paradigm of Hajij et al. (2023b) provides a unifying framework for TNNs, and all networks used in TopoBench can be viewed as special cases of this approach.

Definition 10 (*k*-cochain spaces) Let $\mathcal{C}^k(\mathcal{X}, \mathbb{R}^d)$ be the \mathbb{R} -vector space of functions \mathbf{H}_k where $\mathbf{H}_k: \mathcal{X}^k \rightarrow \mathbb{R}^d$ for a rank $k \in \mathbb{Z}_{\geq 0}$. This space is called the *k-cochain space*, and elements \mathbf{H}_k in $\mathcal{C}^k(\mathcal{X}, \mathbb{R}^d)$ are the *k-cochains* (or *k-signals*).

A *k-cochain* is thus a feature vector associated with each *k-cell*. For a graph, 0-cochains correspond to node features, and 1-cochains correspond to edge features.

Definition 11 (TNN) Let \mathcal{X} be a topological domain. Suppose $\mathcal{C}^{i_1} \times \dots \times \mathcal{C}^{i_m}$ and $\mathcal{C}^{j_1} \times \dots \times \mathcal{C}^{j_n}$ are Cartesian products of cochain spaces on \mathcal{X} . A **topological neural network (TNN)** is a function

$$TNN: \mathcal{C}^{i_1} \times \dots \times \mathcal{C}^{i_m} \longrightarrow \mathcal{C}^{j_1} \times \dots \times \mathcal{C}^{j_n}.$$

A TNN takes as input a collection of cochains $(\mathbf{H}_{i_1}, \dots, \mathbf{H}_{i_m})$ and produces a collection $(\mathbf{K}_{j_1}, \dots, \mathbf{K}_{j_n})$. To enable data exchange within a topological domain, one relies on *cochain maps* (e.g., incidence or adjacency matrices) and *neighborhood functions*, described next.

Cochain maps are fundamental operators for data manipulation in topological domains. For $r < k$, incidence matrices $B_{r,k}$ and adjacency matrices $A_{r,k}$ define mappings:

$$B_{r,k} : \mathcal{C}^k(\mathcal{X}) \rightarrow \mathcal{C}^r(\mathcal{X}), \quad A_{r,k} : \mathcal{C}^r(\mathcal{X}) \rightarrow \mathcal{C}^k(\mathcal{X}).$$

They collectively redistribute signals across different dimensional cells.

Definition 12 (Neighborhood function) *Let S be a nonempty set. A **neighborhood function** on S is a function $\mathcal{N} : S \rightarrow \mathcal{P}(\mathcal{P}(S))$ that assigns to each point x in S a nonempty collection $\mathcal{N}(x)$ of subsets of S . The elements of $\mathcal{N}(x)$ are called **neighborhoods** of x with respect to \mathcal{N} .*

Here, \mathcal{P} denotes the power set operator, where $\mathcal{P}(S)$ is the set of all subsets of S . Thus, $\mathcal{P}(\mathcal{P}(S))$ represents the set of all collections of subsets of S . This formulation enables the assignment of multiple, potentially overlapping neighborhoods to each point, providing the necessary flexibility to describe diverse neighborhood structures across various topological domains.

The flexibility of neighborhood functions is crucial for representing complex relationships in higher-order topological structures, where elements may exhibit multifaceted connections or interactions. By generalizing the concept of node neighborhoods from graphs to higher-order structures, these functions define how information propagates between different elements in the topological domain. This generalization forms the foundation for extending traditional graph-based algorithms to more complex topological spaces, enabling the modeling of sophisticated relational data.

A.4 Traditional Message Passing on Graphs

GNNs have emerged as a powerful class of models for processing graph-structured data. While numerous variations of GNN architectures exist Veličković et al. (2018), at their core lies an iterative message passing algorithm that propagates information between the nodes of the graph. This process can be understood in terms of the basic concepts we introduced earlier.

Formally, a graph is defined as a tuple of nodes and edges, $\mathcal{G} = (\mathcal{V}, \mathcal{E})$. In the context of k-cochain spaces introduced in Section A.3.1, we can view node features as 0-cochains and edge features as 1-cochains. We denote by $h_k^t \in \mathbb{R}^d$ the hidden state of a node k at MP iteration t , which can be seen as an element of a 0-cochain space.

The neighborhood function for a graph, as per Definition 12, is typically defined as $N(k) = \{v \in \mathcal{V} \mid (k, v) \in \mathcal{E}\}$, representing the one-hop neighborhood of each node.

The MP process consists of three main steps:

1. **Message Generation:** Each node k receives messages from all the nodes in its neighborhood $N(k)$. Messages are generated by applying a message function $m(\cdot)$ to the hidden states of node pairs in the graph.
2. **Message Aggregation:** The generated messages are combined using a permutation invariant aggregation function \oplus , as shown in Equation 1. This aggregation can be seen as an application of the neighborhood function concept.

3. **Node Update:** An update function $u(\cdot)$ is used to compute a new hidden state for every node, as shown in Equation 2.

These steps are formalized in the following equations:

$$M_k^{t+1} = \bigoplus_{i \in N(k)} m(h_k^t, h_i^t), \tag{1}$$

$$h_k^{t+1} = u(h_k^t, M_k^{t+1}), \tag{2}$$

where $m(\cdot)$ and $u(\cdot)$ are differentiable functions and consequently may be implemented as neural networks.

This process can be seen as a specific instance of the more general higher-order message passing framework that is introduced in the next section, applied to the case of graphs where we only have 0-cells (nodes) and 1-cells (edges).

A.5 Higher-Order Message Passing

Higher-Order Message Passing (HOMP) generalizes information propagation techniques to complex topological domains such as hypergraphs, simplicial complexes, and cell complexes. This section introduces a formal framework for HOMP, building on the foundational concepts of k-cochain spaces and neighborhood functions defined earlier. By leveraging the rich relationships captured in these advanced topological representations, this unified approach enables modeling and analyzing intricate multi-way interactions across various topological structures, including both traditional graphs and more complex higher-order domains.

Extending Message Passing to Higher-Order Domains The extension of graph message passing to higher-order domains involves generalizing the concepts of message passing to more complex topological structures. This generalization allows us to capture and process richer relational information that goes beyond pairwise interactions.

In higher-order domains, the notion of a "neighborhood" becomes more complex. Instead of just considering adjacent nodes, we now need to consider relationships between higher-dimensional cells (e.g., edges, faces, volumes). The neighborhood functions we defined earlier play a crucial role in formalizing these complex relationships.

Higher-Order Message Passing Framework With k-cochain spaces providing a way to represent data and neighborhood functions defining relationships, we can now formally define the HOMP procedure. Let \mathcal{X} be a topological domain, and let $\mathcal{N} = \{\mathcal{N}_1, \dots, \mathcal{N}_n\}$ be a set of neighborhood functions defined on \mathcal{X} . Consider a cell x and another cell $y \in \mathcal{N}_k(x)$ for some $\mathcal{N}_k \in \mathcal{N}$. A message $m_{x,y}$ between cells x and y is a computation depending on these two cells or on the data they support. Let $\mathcal{N}(x)$ denote the multi-set $\{\!\!\{\mathcal{N}_1(x), \dots, \mathcal{N}_n(x)\}\!\!\}$, and

let $h_x^{(l)}$ represent the data supported on the cell x at layer l . HOMP is defined as follows:

$$m_{x,y} = \alpha_{\mathcal{N}_k}(h_x^{(l)}, h_y^{(l)}), \quad (3)$$

$$m_x^k = \bigoplus_{y \in \mathcal{N}_k(x)} m_{x,y}, \quad 1 \leq k \leq n, \quad (4)$$

$$m_x = \bigotimes_{\mathcal{N}_k \in \mathcal{N}(x)} m_x^k, \quad (5)$$

$$h_x^{(l+1)} = \beta(h_x^{(l)}, m_x). \quad (6)$$

where \bigoplus is a permutation-invariant aggregation function, which is referred to as intra-neighborhood aggregation of x , and \bigotimes , is an aggregation function called the inter-neighborhood aggregation of x . The functions $\alpha_{\mathcal{N}_k}$ and β are differentiable functions.

To summarize the HOMP process:

- **Message Generation:** $m_{x,y}$ is the message computed from x to y using the function $\alpha_{\mathcal{N}_k}$.
- **Message Aggregation (intra):** m_x^k aggregates all messages from the neighbors y in the neighborhood $\mathcal{N}_k(x)$ using the intra-neighborhood function \bigoplus .
- **Message Aggregation (inter):** m_x further aggregates these results across all neighborhoods $\mathcal{N}_k \in \mathcal{N}(x)$ using the inter-neighborhood function \bigotimes .
- **Cell Update:** $h_x^{(l+1)}$ updates the data on cell x by combining its current data $h_x^{(l)}$ with the aggregated message m_x using the function β .

This framework allows for rich information exchange across different dimensions and types of relationships in the topological domain, enabling the modeling of complex, multi-way interactions in various real-world systems.

Appendix B. Implemented Liftings

This appendix provides a detailed overview of the structural liftings currently implemented within **TopoBench**. Table 3 presents each implemented lifting as a row, specifying the source and destination topological domains involved. Additionally, each row indicates whether the lifting is feature-based or connectivity-based. For an intuitive understanding of these lifting types, please refer to the informal definitions in Section 4.3. For a rigorous mathematical treatment of lifting definitions and their taxonomy, please consult Appendix A.2.

Table 3: List of implemented liftings, each one linked with its description. The domains are: PC for point clouds, G for graphs, HG for hypergraphs, SC for simplicial complexes, CC for cellular complexes, and CCC for combinatorial complexes.

Lifting name	Source	Dest.	Feat.-based	Conn.-based
Clique	G	SC		✓
Neighborhood	G	SC		✓
Vietoris-Rips	G	SC	✓	
Graph induced	G	SC		✓
Line	G	SC		✓
Eccentricity	G	SC		✓
DnD	G	SC	✓	
Random latent clique	G	SC		✓
Neighborhood complex	G	SC		✓
Alpha complex	PC	SC	✓	
Random flag complex	PC	SC		✓
Cycle	G	CC		✓
Discrete configuration	G	CC		✓
K-hop	G	HG		✓
Expander hypergraph	G	HG		✓
KNN	G	HG		✓
Kernel	G	HG	✓	✓
Mapper	G	HG		✓
Modularity maximization	G	HG	✓	✓
Forman-Ricci curvature	G	HG		✓
Voronoi	PC	HG	✓	
PointNet++	PC	HG	✓	
Mixture of Gaussians + MST	PC	HG	✓	
Simplicial paths	G	CCC		✓
Coface	SC	CCC		✓
Universal strict	HG	CCC		✓

Lastly, we refer to the [TopoBench Wiki](#) to get a full list of compatible structural liftings from the ICML 2024 TDL Challenge (Bernárdez et al., 2024).

Appendix C. Further Experimental Details

This appendix provides details on the hyperparameter search methodology, optimization strategy, computational resources used for the experiments, and additional results and analyses.

C.1 Experiment Configuration and Model Execution

To automate the configuration of `TopoBench` modules, the `hydra` package (Yadan, 2019) is employed. In particular, hierarchical configuration groups and registers facilitate easy use of the library: there is no need to meticulously select each module for any given domain. Simply choosing a dataset and a model automatically configures a full default pipeline, eliminating the need for manual intervention. Model execution and training are further automated by the `lightning` library (Lisa and Bot, 2017), which orchestrates training, validation, and testing while also handling logging and callbacks.

C.2 Hyperparameter Search

Five splits are generated for each dataset to ensure a fair evaluation across domains, allocating 50% of data for training, 25% for validation, and 25% for testing. An exception is made for the ZINC dataset, which uses predefined splits (Irwin et al., 2012).

Each model (in each domain) has numerous specific hyperparameters that can be tuned to enhance performance. TNNs, in particular, come with additional parameters that could further boost results. To avoid the combinatorial explosion of all possible hyperparameter sets, the search space is restricted to hyperparameters common across every model. A grid-search strategy is used to identify the optimal parameters for each model-dataset combination. Specifically, the encoder hidden dimension is varied over $\{32, 64, 128\}$, the encoder dropout over $\{0.25, 0.5\}$, the number of backbone layers over $\{1, 2, 3, 4\}$, the learning rate over $\{0.01, 0.001\}$, and the batch size over $\{128, 256\}$. For models in the cellular and simplicial domains, the readout type is also varied between direct readout (DR) and signal down-propagation (SDP). If a model exceeds available GPU memory, the batch size, encoder hidden dimension, and number of backbone layers are reduced until training becomes feasible.

For node-level tasks, validation is conducted after each training epoch, continuing until either the maximum number of epochs is reached or the optimization metric fails to improve for 50 consecutive validation epochs; a minimum of 50 epochs is always enforced. For graph-level tasks, validation is performed every 5 epochs, halting early if validation performance fails to improve for 10 consecutive checks. The optimization uses `torch.optim.Adam` combined with `torch.optim.lr_scheduler.StepLR`, where the step size is 50 and $\gamma = 0.5$. Over 100,000 runs have been executed to obtain the final results. In general, the best hyperparameter set is selected based on the highest average performance across the five validation splits. For ZINC, five different initialization seeds are used to obtain an average performance.

All experiments are conducted on a Linux machine equipped with 256 CPU cores, 1TB of system memory, and 8 NVIDIA A30 GPUs, each with 24GB of GPU memory.

C.3 Descriptive Summaries of Datasets

Table 4 provides descriptive statistics for each dataset used in the numerical experiments (see Section 5 for details) after lifting to three topological domains: simplicial complexes, cellular complexes, and hypergraphs. The columns labeled 0-cell, 1-cell, 2-cell, and 3-cell show the count of each n -cell in the resulting dataset. Specifically, a clique complex lifting is applied to obtain a simplicial domain with a maximum dimension of three, cycle-based

lifting is used to obtain a cellular domain with a maximum dimension of two, and k -hop lifting (with $k = 1$) is used to lift each graph into a hypergraph.

Table 5 reports additional descriptive statistics for the graph datasets used in the experiments. Specifically, the table includes the dimensionality of the number of classes (set to 1 for regression tasks and to the actual class count for classification tasks), and the number of graphs in each dataset and the initial 0-cell (node) features. Note that, for the illustrative experiments in Section 5, a projected sum feature lifting is applied. Consequently, higher-order cells (e.g., 1-cells, 2-cells, etc.) inherit the same initial feature dimensionality as the 0-cells.

C.4 Additional Results and Analysis

Table 6 additionally presents results for the CCXN and SCCN networks, which on average perform slightly worse than other models. As shown in Table C.4, the CCXN network performs better when using SDP readout, though not as dramatically as CWN under the same strategy. The SCCN model benefits more from SDP readout than other simplicial-domain models (SCN and SCCNN), showing improvements in 9 out of 21 cases, whereas SCCNN and SCN show improvements in 3 and 5 cases, respectively. Overall, cellular models demonstrate improved performance on 15, 19, and 8 datasets for CCXN, CWN, and CCCN, respectively, when using SDP. In contrast, simplicial models achieve 9, 3, and 5 improvements for SCCN, SCCNN, and SCN, respectively, with the same readout.

Note that for demonstration purposes, only one fixed lifting is applied to transform graphs into each of the considered topological domains, leaving a domain-specific optimal lifting strategy beyond the scope of this paper.⁵ Specifically, a clique complex is used for simplicial lifting, cycle-based lifting is used for cellular domains, and k -hop lifting (with $k = 1$) is used for hypergraphs. Feature projection is also applied, where the $(n - 1)$ -cell features are multiplied by the corresponding incidence matrices to generate n -cell features.

Finally, Tables 8 and 9 present the number of learnable parameters for each best-performing model configuration and their corresponding runtimes. Overall, these results indicate that TNNs tend to be less efficient in terms of memory usage and computational time compared to their graph-based counterparts. However, there are exceptions: EDGNN and UniGNN2 achieve parameter counts comparable to graph baselines, and among the TNNs, AST and EDGNN stand out as the most efficient on average.

Appendix D. Higher-Order Datasets

D.1 Descriptive Summaries of Higher-Order Datasets

Tables 11 and 12 provide descriptive summaries of the higher-order datasets included in TopoBench, which spans 13 datasets drawn from a broad range of hypergraph and simplicial benchmark sources.

Hypergraph datasets: For the co-authorship networks (Cora-CA and DBLP-CA) and co-citation networks (Cora, Citeseer, and Pubmed), we use the versions provided by Yadati et al. (2019). For 3D object classification, we include the Princeton ModelNet40 (Wu et al., 2015) and National Taiwan University (Chen et al., 2003) datasets, with hypergraphs

5. Learnable liftings may further optimize the predictive capacity of higher-order networks.

Table 4: Descriptive summaries of the datasets used in the experiments.

Dataset	Domain	0-cell	1-cell	2-cell	3-cell	Num. Hyperedges
Cora	Cellular	2708	5278	2648	0	0
	Simplicial	2708	5278	1630	220	0
	Hypergraph	2708	0	0	0	2708
Citeseer	Cellular	3327	4552	1663	0	0
	Simplicial	3327	4552	1167	255	0
	Hypergraph	3327	0	0	0	3327
PubMed	Cellular	19717	44324	23605	0	0
	Simplicial	19717	44324	12520	3275	0
	Hypergraph	19717	0	0	0	19717
MUTAG	Cellular	3371	3721	538	0	0
	Simplicial	3371	3721	0	0	0
	Hypergraph	3371	0	0	0	3371
NCI1	Cellular	122747	132753	14885	0	0
	Simplicial	122747	132753	186	0	0
	Hypergraph	122747	0	0	0	122747
NCI109	Cellular	122494	132604	15042	0	0
	Simplicial	122494	132604	183	0	0
	Hypergraph	122494	0	0	0	122494
PROTEINS	Cellular	43471	81044	38773	0	0
	Simplicial	43471	81044	30501	3502	0
	Hypergraph	43471	0	0	0	43471
REDDIT-BINARY	Cellular	859254	995508	141218	0	0
	Simplicial	859254	995508	49670	1303	0
	Hypergraph	859254	0	0	0	859254
IMDB-BINARY	Cellular	19773	96531	77758	0	0
	Simplicial	19773	96531	391991	1694513	0
	Hypergraph	19773	0	0	0	19773
IMDB-MULTI	Cellular	19502	98903	80901	0	0
	Simplicial	19502	98903	458850	2343676	0
	Hypergraph	19502	0	0	0	19502
ZINC	Cellular	277864	298985	33121	0	0
	Simplicial	277864	298985	769	0	0
	Hypergraph	277864	0	0	0	277864
Amazon Ratings	Cellular	24492	93050	68553	0	0
	Simplicial	24492	93050	110765	64195	0
	Hypergraph	24492	0	0	0	24492
Minesweeper	Cellular	10000	39402	28955	0	0
	Simplicial	10000	39402	39204	9801	0
	Hypergraph	10000	0	0	0	10000
Roman Empire	Cellular	22662	32927	10266	0	0
	Simplicial	22662	32927	7168	0	0
	Hypergraph	22662	0	0	0	22662
Tolokers	Cellular	OOM	OOM	OOM	OOM	OOM
	Simplicial	OOM	OOM	OOM	OOM	OOM
	Hypergraph	11758	0	0	0	11758
US-county-demos	Cellular	3224	9483	6266	0	0
	Simplicial	3224	9483	6490	225	0
	Hypergraph	3224	0	0	0	3224

Table 5: Additional descriptive statistics of the graph datasets used in the experiments.

	Dataset	0-cell dim	Num. classes	Num. graphs
Graph	Cora	1433	7	1
	Citeseer	3703	6	1
	PubMed	19717	500	3
	MUTAG	7	2	188
	NCI1	37	2	4110
	NCI109	38	2	4127
	PROTEINS	3	2	1113
	REDDIT-BINARY	10	2	2000
	IMDB-BINARY	136	2	1000
	IMDB-MULTI	89	3	1500
	ZINC	21	1	12000
	Amazon Ratings	300	5	1
	Minesweeper	7	2	1
	Roman Empire	300	18	1
	Tolokers	10	2	1
	US-county-demos	6	1	1

Table 6: Cross-domain comparison: results are shown as mean and standard deviation. The best result is bold and shaded in grey, while those within one standard deviation are in blue-shaded boxes.

Dataset	GCN	GIN	GAT	AST	EDGNN	UniGNN2	CCXN	CWN	CCCN	SCCN	SCCNCN	SCN		
Node-level tasks	Cora	87.09 ± 0.2	87.21 ± 1.89	86.71 ± 0.95	88.92 ± 0.44	87.06 ± 1.09	86.97 ± 0.88	86.79 ± 1.81	86.32 ± 1.38	87.44 ± 1.28	80.86 ± 2.16	82.19 ± 1.07	82.27 ± 1.34	
	Citeseer	75.53 ± 1.27	73.73 ± 1.23	74.41 ± 1.75	73.85 ± 2.21	74.93 ± 1.39	74.72 ± 1.08	74.67 ± 2.24	75.2 ± 1.82	75.63 ± 1.58	69.6 ± 1.83	70.23 ± 2.69	71.24 ± 1.68	
	PubMed	89.4 ± 0.3	89.29 ± 0.41	89.44 ± 0.24	89.62 ± 0.25	89.04 ± 0.51	89.34 ± 0.45	88.91 ± 0.47	88.64 ± 0.36	88.52 ± 0.44	88.37 ± 0.48	88.18 ± 0.32	88.72 ± 0.5	
	Amazon	49.56 ± 0.55	49.16 ± 1.02	50.17 ± 0.59	50.5 ± 0.27	48.18 ± 0.09	49.06 ± 0.08	48.93 ± 0.14	51.9 ± 0.15	50.26 ± 0.17	OOM	OOM	OOM	
	Empire	78.16 ± 0.32	79.56 ± 0.2	84.02 ± 0.51	79.5 ± 0.13	81.01 ± 0.24	77.06 ± 0.2	81.44 ± 0.31	81.81 ± 0.62	82.14 ± 0.0	88.27 ± 0.14	89.15 ± 0.32	88.79 ± 0.46	
	Minesweeper	87.52 ± 0.42	87.82 ± 0.34	89.64 ± 0.43	81.14 ± 0.05	84.52 ± 0.05	78.02 ± 0.0	88.88 ± 0.36	88.62 ± 0.04	89.42 ± 0.0	89.07 ± 0.25	89.0 ± 0.0	90.32 ± 0.11	
	Tolokers	83.02 ± 0.71	80.72 ± 1.19	84.43 ± 1.0	83.26 ± 0.1	77.53 ± 0.01	77.35 ± 0.03	OOM	OOM	OOM	OOM	OOM	OOM	
	Election	0.31 ± 0.02	0.28 ± 0.02	0.29 ± 0.02	0.29 ± 0.01	0.34 ± 0.02	0.37 ± 0.02	0.35 ± 0.02	0.34 ± 0.02	0.31 ± 0.02	0.53 ± 0.03	0.51 ± 0.03	0.46 ± 0.04	
	Bachelor	0.29 ± 0.02	0.31 ± 0.03	0.28 ± 0.02	0.3 ± 0.03	0.29 ± 0.02	0.31 ± 0.02	0.32 ± 0.03	0.33 ± 0.03	0.31 ± 0.02	0.36 ± 0.02	0.34 ± 0.03	0.32 ± 0.02	
	Birth	0.72 ± 0.09	0.72 ± 0.09	0.71 ± 0.09	0.71 ± 0.08	0.7 ± 0.07	0.73 ± 0.1	0.74 ± 0.11	0.72 ± 0.09	0.71 ± 0.09	0.82 ± 0.09	0.79 ± 0.12	0.71 ± 0.08	
	Death	0.51 ± 0.04	0.52 ± 0.04	0.51 ± 0.04	0.49 ± 0.05	0.52 ± 0.05	0.51 ± 0.05	0.54 ± 0.06	0.54 ± 0.06	0.54 ± 0.06	0.58 ± 0.06	0.55 ± 0.05	0.52 ± 0.05	
	Income	0.22 ± 0.03	0.21 ± 0.02	0.2 ± 0.02	0.21 ± 0.02	0.23 ± 0.02	0.23 ± 0.02	0.25 ± 0.03	0.25 ± 0.03	0.23 ± 0.02	0.29 ± 0.03	0.28 ± 0.03	0.25 ± 0.02	
	Migration	0.8 ± 0.12	0.8 ± 0.1	0.77 ± 0.13	0.78 ± 0.12	0.8 ± 0.12	0.79 ± 0.12	0.85 ± 0.18	0.84 ± 0.13	0.84 ± 0.12	0.91 ± 0.18	0.9 ± 0.14	0.92 ± 0.2	
	Unempl	0.25 ± 0.03	0.22 ± 0.02	0.23 ± 0.03	0.22 ± 0.02	0.26 ± 0.03	0.28 ± 0.02	0.27 ± 0.03	0.25 ± 0.03	0.24 ± 0.03	0.43 ± 0.04	0.43 ± 0.04	0.38 ± 0.04	
	Graph-level tasks	MUTAG	69.79 ± 6.8	79.57 ± 6.13	72.77 ± 2.77	71.06 ± 6.49	80.0 ± 4.9	80.43 ± 4.09	74.89 ± 5.51	80.43 ± 1.78	77.02 ± 9.32	70.64 ± 5.9	76.17 ± 6.63	73.62 ± 6.13
		PROTEINS	75.7 ± 2.14	75.2 ± 3.3	76.34 ± 1.66	76.63 ± 1.74	73.91 ± 4.39	75.2 ± 2.96	75.63 ± 2.57	76.13 ± 2.7	73.33 ± 2.3	75.05 ± 2.76	74.19 ± 2.86	75.27 ± 2.14
NCI1		72.86 ± 0.69	74.26 ± 0.96	75.0 ± 0.99	75.18 ± 1.24	73.97 ± 0.82	73.02 ± 0.92	74.86 ± 0.82	73.93 ± 1.87	76.67 ± 1.48	76.17 ± 1.39	76.6 ± 1.75	74.49 ± 1.04	
NCI109		72.2 ± 1.22	74.42 ± 0.7	73.8 ± 0.73	73.75 ± 1.09	74.93 ± 2.5	70.76 ± 1.11	75.66 ± 1.3	73.8 ± 2.06	75.35 ± 1.5	75.49 ± 1.39	77.12 ± 1.07	75.7 ± 1.04	
IMDB-BIN		72.0 ± 2.48	70.96 ± 1.93	69.76 ± 2.65	70.32 ± 3.27	69.12 ± 2.92	71.04 ± 1.31	70.08 ± 1.21	70.4 ± 2.02	69.12 ± 2.82	70.88 ± 3.98	70.88 ± 2.25	70.8 ± 2.38	
IMDB-MUL		49.97 ± 2.16	47.68 ± 4.21	50.13 ± 3.87	50.51 ± 2.92	49.17 ± 4.35	49.76 ± 3.55	47.63 ± 3.45	49.71 ± 2.83	47.79 ± 3.45	49.71 ± 3.7	48.75 ± 3.98	49.49 ± 5.08	
REDDIT		76.24 ± 0.54	81.96 ± 1.36	75.68 ± 1.0	74.84 ± 2.68	83.24 ± 1.45	75.56 ± 3.19	82.84 ± 2.54	85.52 ± 1.38	85.12 ± 1.29	74.44 ± 1.74	77.24 ± 1.87	71.28 ± 2.06	
ZINC		0.62 ± 0.01	0.57 ± 0.04	0.61 ± 0.01	0.59 ± 0.02	0.51 ± 0.01	0.6 ± 0.01	0.4 ± 0.04	0.34 ± 0.01	0.34 ± 0.02	0.46 ± 0.08	0.36 ± 0.02	0.53 ± 0.04	

constructed following the protocols in Feng et al. (2019) and Yang et al. (2020), using both MVCNN (Su et al., 2015) and GVCNN (Feng et al., 2019) features. Additionally, we evaluate performance on three datasets with categorical attributes—20NewsGroups, Mushroom, and ZOO—sourced from the UCI Categorical Machine Learning Repository (Dua et al., 2017). For these, we construct hypergraphs as in Yadati et al. (2019), where a hyperedge is formed by grouping data points sharing the same categorical feature value.

Table 11 summarizes the statistics of the hypergraph datasets along with their associated homophily metrics: clique-expansion homophily (Wang et al., 2023) and Δ -homophily (Telyatnikov et al., 2025). These measures capture the degree to which hyperedges align with label

Table 7: Ablation study comparing the performance of CCXN, CWN, CCCN, SCCN, SC-CNN, and SCN models on various datasets using two readout strategies, direct readout (DR) and signal down-propagation (SDP). SDP generally enhances CWN performance, whereas the effect of SDP on CCCN, SCCNN, and SCN varies based on their internal signal propagation mechanisms. Means and standard deviations of performance metrics are shown. The best results are shown in bold for each model and readout type.

Dataset	CCXN		CWN		CCCN		SCCN		SCCNN		SCN	
	DR	SDP	DR	SDP	DR	SDP	DR	SDP	DR	SDP	DR	SDP
Cora	86.32 ± 1.22	86.79 ± 1.81	74.95 ± 0.98	86.32 ± 1.38	87.44 ± 1.28	87.68 ± 1.17	80.86 ± 2.16	80.06 ± 1.66	82.19 ± 1.07	80.65 ± 2.39	82.27 ± 1.34	79.91 ± 1.18
Citeseer	72.87 ± 1.13	74.67 ± 2.24	70.49 ± 2.85	75.2 ± 1.82	75.63 ± 1.58	74.91 ± 1.25	69.6 ± 1.83	68.86 ± 2.40	70.23 ± 2.69	69.03 ± 2.01	71.24 ± 1.68	70.4 ± 1.53
Pubmed	88.91 ± 0.47	88.38 ± 0.38	86.94 ± 0.68	88.64 ± 0.36	88.52 ± 0.44	88.67 ± 0.39	88.04 ± 0.51	88.37 ± 0.48	88.18 ± 0.32	87.78 ± 0.58	88.72 ± 0.5	88.62 ± 0.44
Amazon	48.93 ± 0.14	48.34 ± 0.12	45.58 ± 0.25	51.9 ± 0.15	50.55 ± 0.15	50.26 ± 0.17	OOM	OOM	OOM	OOM	OOM	OOM
Empire	80.46 ± 0.23	81.44 ± 0.31	66.13 ± 0.03	81.81 ± 0.62	82.14 ± 0.00	82.51 ± 0.0	88.2 ± 0.22	88.27 ± 0.14	89.15 ± 0.32	88.73 ± 0.12	85.89 ± 0.34	88.79 ± 0.46
Minesweeper	88.88 ± 0.36	89.76 ± 0.32	48.82 ± 0.0	88.62 ± 0.04	89.42 ± 0.00	89.85 ± 0.00	88.85 ± 0.00	89.07 ± 0.25	87.4 ± 0.0	89.0 ± 0.00	90.32 ± 0.11	90.27 ± 0.36
Election	0.39 ± 0.05	0.35 ± 0.02	0.6 ± 0.04	0.34 ± 0.02	0.31 ± 0.02	0.31 ± 0.01	0.53 ± 0.03	0.57 ± 0.02	0.51 ± 0.03	0.56 ± 0.04	0.46 ± 0.04	0.51 ± 0.03
Bachelor	0.33 ± 0.03	0.32 ± 0.03	0.33 ± 0.03	0.33 ± 0.03	0.32 ± 0.02	0.31 ± 0.02	0.36 ± 0.02	0.34 ± 0.02	0.34 ± 0.03	0.34 ± 0.03	0.32 ± 0.02	0.32 ± 0.03
Birth	0.80 ± 0.12	0.74 ± 0.11	0.81 ± 0.11	0.72 ± 0.09	0.71 ± 0.09	0.72 ± 0.05	0.82 ± 0.09	0.83 ± 0.10	0.79 ± 0.12	0.83 ± 0.12	0.71 ± 0.08	0.8 ± 0.11
Death	0.57 ± 0.06	0.54 ± 0.06	0.55 ± 0.05	0.54 ± 0.06	0.54 ± 0.06	0.54 ± 0.06	0.58 ± 0.06	0.56 ± 0.04	0.55 ± 0.05	0.58 ± 0.05	0.52 ± 0.05	0.56 ± 0.05
Income	0.25 ± 0.03	0.27 ± 0.03	0.36 ± 0.04	0.25 ± 0.03	0.23 ± 0.02	0.23 ± 0.02	0.29 ± 0.03	0.29 ± 0.03	0.28 ± 0.03	0.31 ± 0.03	0.25 ± 0.02	0.27 ± 0.02
Migration	0.80 ± 0.11	0.85 ± 0.18	0.9 ± 0.16	0.84 ± 0.13	0.84 ± 0.10	0.84 ± 0.10	0.91 ± 0.18	0.93 ± 0.17	0.90 ± 0.14	0.93 ± 0.17	0.92 ± 0.20	0.96 ± 0.23
Unempl	0.28 ± 0.05	0.27 ± 0.03	0.46 ± 0.04	0.25 ± 0.03	0.24 ± 0.03	0.25 ± 0.03	0.43 ± 0.04	0.47 ± 0.04	0.43 ± 0.04	0.45 ± 0.04	0.38 ± 0.04	0.41 ± 0.03
MUTAG	69.79 ± 4.61	74.89 ± 5.51	69.68 ± 8.58	80.43 ± 1.78	80.85 ± 5.42	77.02 ± 9.32	70.64 ± 5.90	73.62 ± 4.41	76.17 ± 6.63	70.64 ± 3.16	71.49 ± 2.43	73.62 ± 6.13
PROTEINS	75.63 ± 2.57	74.91 ± 1.85	76.13 ± 1.80	76.13 ± 2.70	73.55 ± 3.43	73.33 ± 2.30	75.05 ± 2.76	74.34 ± 3.17	74.19 ± 2.86	74.98 ± 1.92	75.27 ± 2.14	74.77 ± 1.69
NCII	72.43 ± 1.72	74.86 ± 0.82	68.52 ± 0.51	73.93 ± 1.87	76.67 ± 1.48	77.65 ± 1.28	76.42 ± 0.88	76.17 ± 1.39	76.6 ± 1.75	75.6 ± 2.45	75.27 ± 1.57	74.49 ± 1.03
NCII09	73.22 ± 0.48	75.66 ± 1.30	68.19 ± 0.65	73.8 ± 2.06	75.35 ± 1.50	74.83 ± 1.18	75.49 ± 1.39	75.31 ± 1.36	77.12 ± 1.07	75.43 ± 1.94	74.58 ± 1.29	75.7 ± 1.04
IMDB-BIN	70.08 ± 1.21	68.96 ± 2.03	70.4 ± 2.02	69.28 ± 2.57	69.12 ± 2.82	69.44 ± 2.46	70.88 ± 3.98	69.76 ± 3.16	70.88 ± 2.25	69.28 ± 5.69	70.8 ± 2.38	68.64 ± 3.90
IMDB-MUL	47.63 ± 3.45	48.75 ± 3.56	49.71 ± 2.83	49.87 ± 2.33	49.01 ± 2.63	47.79 ± 3.45	49.71 ± 3.70	47.31 ± 3.12	48.75 ± 3.98	46.67 ± 3.13	48.16 ± 2.89	49.49 ± 5.08
REDDIT	74.40 ± 1.50	82.84 ± 2.54	76.20 ± 0.86	85.52 ± 1.38	85.12 ± 1.29	83.32 ± 0.73	74.16 ± 1.54	74.44 ± 1.74	75.56 ± 3.46	77.24 ± 1.87	71.28 ± 2.06	69.68 ± 4.0
ZINC	0.63 ± 0.02	0.40 ± 0.04	0.70 ± 0.0	0.34 ± 0.01	0.35 ± 0.02	0.34 ± 0.02	0.55 ± 0.01	0.46 ± 0.08	0.36 ± 0.01	0.36 ± 0.02	0.59 ± 0.01	0.53 ± 0.04

Table 8: Model sizes corresponding to the best set of hyperparameters

Model	GCN	GAT	GIN	AST	EDGNN	UniGNN2	CWN	CCCN	CCXN	SCN	SCCN	SCCNN
Cora	234.63K	113.61K	105.03K	60.26K	113.29K	109.06K	343.11K	451.85K	735.37K	144.62K	155.88K	164.17K
Citeseer	525.06K	558.60K	122.05K	132.87K	258.50K	541.32K	1754.50K	1032.84K	758.41K	737.29K	782.34K	893.13K
Pubmed	114.69K	148.23K	53.38K	280.83K	147.59K	114.56K	163.72K	85.76K	277.51K	134.40K	457.99K	605.06K
MUTAG	67.97K	22.02K	38.40K	80.77K	5.73K	84.10K	334.72K	284.29K	73.86K	20.03K	398.85K	27.11K
PROTEINS	13.19K	10.11K	13.19K	14.34K	5.60K	21.31K	101.12K	34.56K	86.53K	10.24K	307.31K	26.72K
NCII	6.72K	11.20K	154.37K	57.47K	88.19K	104.32K	124.10K	63.87K	15.87K	94.98K	131.84K	188.99K
NCII09	23.75K	11.23K	154.50K	221.57K	88.32K	4.61K	412.29K	17.67K	17.36K	26.08K	135.75K	49.54K
IMDB-BIN	21.70K	21.83K	9.89K	114.24K	9.86K	100.61K	68.80K	218.24K	19.04K	202.63K	563.07K	285.83K
IMDB-MUL	62.08K	6.37K	18.76K	111.30K	27.01K	8.32K	19.68K	45.64K	56.26K	5.45K	145.16K	121.22K
REDDIT	13.63K	30.66K	10.08K	106.18K	5.83K	68.10K	26.66K	47.94K	57.54K	7.84K	69.31K	286.59K
Amazon	122.37K	156.16K	89.35K	155.91K	122.24K	89.22K	578.95K	310.15K	200.96K	OOM	OOM	OOM
Minesweeper	9.28K	5.89K	51.46K	118.02K	21.70K	51.33K	22.24K	35.07K	8.83K	51.97K	25.15K	33.44K
Empire	37.39K	41.81K	33.23K	257.17K	41.49K	90.90K	142.74K	86.10K	43.83K	415.89K	612.50K	240.53K
Tolokers	84.87K	151.94K	3.75K	217.99K	21.89K	13.57K	12.07K	OOM	OOM	OOM	OOM	OOM
Election	84.22K	151.30K	150.27K	217.34K	21.57K	4.58K	118.08K	234.37K	253.18K	16.64K	11.52K	415.10K
Bachelor	17.47K	151.30K	7.81K	316.93K	84.10K	3.55K	43.78K	34.88K	42.86K	27.14K	43.52K	415.10K
Birth	4.64K	30.34K	5.70K	30.21K	84.10K	13.25K	26.24K	22.40K	253.18K	103.42K	11.52K	26.98K
Death	21.63K	10.18K	7.81K	316.93K	84.10K	51.07K	26.24K	15.58K	12.86K	27.14K	11.52K	415.10K
Income	17.47K	151.30K	9.92K	217.34K	21.57K	4.58K	85.18K	12.42K	12.86K	27.14K	268.03K	105.15K
Migration	67.71K	10.18K	38.27K	80.64K	21.57K	51.07K	26.24K	15.58K	65.15K	16.64K	11.52K	415.10K
Unempl	84.22K	151.30K	117.25K	105.86K	21.57K	5.60K	101.63K	234.37K	286.46K	27.14K	11.52K	105.15K
ZINC	22.59K	22.85K	10.40K	106.82K	22.53K	102.14K	88.06K	287.74K	16.48K	24.42K	617.86K	1453.82K
Average size	75K ± 111K	89K ± 119K	54K ± 53K	150K ± 88K	59K ± 60K	74K ± 109K	210K ± 367K	170K ± 229K	158K ± 212K	107K ± 172K	263K ± 251K	313K ± 340K

Table 9: Model runtime in seconds corresponding to the best set of hyperparameters

Model	GCN	GAT	GIN	AST	EDGNN	UniGNN2	CWN	CCCN	CCXN	SCN	SCCN	SCCNN
Cora	19.71 ± 3.18	33.51 ± 6.33	24.24 ± 7.48	40.23 ± 11.82	28.17 ± 3.97	35.28 ± 5.14	48.49 ± 27.38	39.36 ± 6.72	35.74 ± 2.93	51.53 ± 14.0	84.04 ± 13.39	65.62 ± 23.49
Citeseer	22.58 ± 2.48	21.18 ± 2.24	24.65 ± 2.58	58.78 ± 2.26	39.59 ± 1.93	41.38 ± 3.55	48.89 ± 4.02	48.39 ± 4.57	53.88 ± 2.81	58.85 ± 18.23	65.33 ± 13.34	80.6 ± 36.39
Pubmed	40.89 ± 8.39	50.2 ± 13.27	59.91 ± 10.56	84.67 ± 13.03	87.25 ± 13.88	160.37 ± 31.88	147.59 ± 28.96	172.63 ± 33.06	212.66 ± 52.26	151.0 ± 22.55	134.82 ± 34.81	171.92 ± 48.25
MUTAG	3.83 ± 0.89	4.16 ± 1.05	4.6 ± 0.56	9.9 ± 3.24	5.81 ± 1.13	5.5 ± 0.78	10.92 ± 0.96	12.04 ± 2.21	10.76 ± 1.89	8.47 ± 2.43	10.71 ± 2.92	14.06 ± 2.51
PROTEINS	8.18 ± 2.47	8.38 ± 2.34	8.88 ± 2.34	15.81 ± 2.89	15.15 ± 3.3	16.78 ± 7.77	53.6 ± 17.7	41.63 ± 7.23	51.98 ± 8.5	42.78 ± 13.41	70.06 ± 15.91	54.13 ± 11.27
NCII	53.23 ± 19.67	57.12 ± 17.49	61.2 ± 23.97	138.13 ± 46.01	110.86 ± 27.75	209.17 ± 11.25	302.34 ± 63.44	372.36 ± 109.47	244.72 ± 46.09	276.32 ± 63.21	332.76 ± 51.89	307.2 ± 83.01
NCII09	37.4 ± 8.63	36.44 ± 9.05	50.32 ± 7.98	138.66 ± 26.38	126.61 ± 45.53	61.25 ± 16.58	294.79 ± 46.27	272.3 ± 20.89	225.72 ± 86.57	226.23 ± 66.29	321.76 ± 55.92	353.09 ± 105.89
IMDB-BIN	8.18 ± 3.33	7.48 ± 2.21	7.72 ± 1.72	21.34 ± 2.96	13.06 ± 4.76	20.75 ± 6.02	61.16 ± 9.33	51.88 ± 12.3	51.2 ± 18.14	374.83 ± 132.68	432.23 ± 57.29	515.13 ± 112.53
IMDB-MUL	10.27 ± 3.58	9.79 ± 1.85	10.42 ± 3.93	20.89 ± 5.05	13.89 ± 3.33	16.74 ± 4.15	39.99 ± 5.18	73.6 ± 20.07	72.3 ± 13.76	776.65 ± 147.42	716.44 ± 232.31	895.77 ± 399.41
REDDIT	16.17 ± 1.75	26.87 ± 5.02	28.75 ± 7.64	72.33 ± 18.33	73.92 ± 26.58	307.4 ± 159.71	1230.53 ± 270.03	1653.47 ± 641.13	1435.07 ± 427.2	985.1 ± 68.42	1622.17 ± 667.71	3670.64 ± 423.25
Amazon	22.12 ± 4.99	25.09 ± 4.41	15.25 ± 2.73	61.77 ± 8.17	52.31 ± 4.88	264.24 ± 29.28	239.31 ± 45.79	149.34 ± 58.59	201.99 ± 38.94	OOM	OOM	OOM
Minesweeper	7.33 ± 1.66	10.64 ± 1.1	8.32 ± 2.51	15.79 ± 2.67	20.4 ± 4.38	58.72 ± 14.39	52.12 ± 13.87	98.2 ± 15.21	50.27 ± 14.89	82.5 ± 14.8	28.76 ± 3.74	54.1 ± 20.66
Empire	23.38 ± 2.21	27.1 ± 1.89	22.36 ± 4.9	82.61 ± 15.26	63.77 ± 13.16	122.23 ± 35.71						

Table 10: TNNs utilized in the experiments and their references

Acronym	Neural network name	Reference
Graph neural networks		
GAT	Graph attention network	Veličković et al. (2018)
GIN	Graph isomorphism network	Xu et al. (2019)
GCN	Semi-Supervised Classification with Graph Convolutional Networks	Kipf and Welling (2016)
Simplicial complexes		
SAN	Simplicial Attention Neural Networks	Giusti et al. (2022)
SCCN	Efficient Representation Learning for Higher-Order Data with Simplicial Complexes	Yang et al. (2022)
SCCNN	Convolutional Learning on Simplicial Complexes	Yang and Isufi (2023)
SCN	Simplicial Complex Neural Networks	Ebli et al. (2020)
Cellular complexes		
CAN	Cell Attention Network	Giusti et al. (2023)
CCCN	Generalized simplicial attention neural networks ⁶	Battiloro et al. (2024b)
CXN	Cell Complex Neural Networks	Hajij et al. (2020)
CWN	Weisfeiler and Lehman Go Cellular: CW Networks	Bodnar et al. (2021a)
Hypergraphs		
AllSetTransformer	You are AllSet: A Multiset Function Framework for Hypergraph Neural Networks	Chien et al. (2021)
EDGNN	Equivariant Hypergraph Diffusion Neural Operators	Wang et al. (2022)
UniGNN	UniGNN: a Unified Framework for Graph and Hypergraph Neural Networks	Huang and Yang (2021)

information, serving as indicators of how well the hypergraph structure supports downstream classification.

Simplicial datasets: In contrast, the MANTRA family (Ballester et al., 2024) comprises purely topological datasets of 2-manifold triangulations. From the suite of tasks it offers, we focus on three representative classification problems: (1) NAME: predicting the homeomorphism class of a triangulated surface, (2) ORIENT: determining its orientability, and (3) β_1, β_2 : predicting the values of the first and second Betti numbers. The task of predicting Betti numbers is performed as a regression, while the outputs are rounded, and then classification metrics are employed to assess performance. Table 12 reports the corresponding dataset statistics for this family.

Table 11: Statistics of hypergraph higher-order datasets

Dataset	0-cell dim	Num. 0-cell	Num. 1-cell	Num. classes	CE Homophily	$\frac{1}{ V } \sum_{v \in V} h_v^0$	$\frac{1}{ V } \sum_{v \in V} h_v^1$
Cora	1433	2708	1579	7	89.74	84.10	78.08
Citeseer	3703	3312	1079	6	89.32	78.25	74.18
Pubmed	500	19717	7963	3	95.24	82.05	75.73
CORA-CA	1433	2708	1072	7	80.26	80.81	76.51
DBLP-CA	1425	41302	22363	6	86.88	88.86	86.01
ZOO	16	101	43	7	82.88	91.13	85.79
20Newsgroups	100	16262	100	4	75.25	81.26	74.78
Mushroom	22	8124	298	2	85.33	88.05	84.41
NTU2012	100	16242	2012	67	46.07	53.24	41.95
ModelNet40	100	12311	12311	40	24.07	42.16	29.42

Table 12: Statistics of MANTRA family simplicial datasets

Dataset	0/1/2-cell dim	Avg. num. 0-cell	Avg. num. 1-cell	Avg. num. 2-cell	Num. classes	Num. objects
NAME	1/1/1	9.98	34.43	22.95	8	43138
ORIENT	1/1/1	9.98	34.43	22.95	2	43138
β_1, β_2	1/1/1	9.98	34.43	22.95	1	43138

D.2 Hypergraph Higher-Order Datasets Results

Table 13 demonstrates varying model effectiveness across real-world classification hypergraph datasets. While no single model consistently outperforms others across all datasets, AllSetTransformer achieves the best performance in 5 out of 10 cases. UniGNN2 achieves top performance on several datasets, including Cora and ModelNet40, while EDGNN leads on CORA-CA and Citeseer. It is important to note that the results shown in Table 13 and Table 1 for Cora, Citeseer, and Pubmed refer to the same base datasets but differ in the nature of their topology. Specifically, the higher-order structures in Table 1 are derived via lifting mechanisms applied to graph data (graph representation of the Cora, Citeseer, and Pubmed), whereas the results in Table 13 are obtained from real hypergraph datasets, where hyperedges are constructed based on available metadata, please refer to Appendix D.2 of Telyatnikov et al. (2025).

Table 13: Test accuracy (mean \pm std) for each hypergraph dataset (rows) and model (columns). The best result is bold and shaded in gray, while those within one standard deviation are in blue-shaded boxes.

	EDGNN	AllSetTransformer	UniGNN2
Cora	78.14 \pm 0.72	78.91 \pm 1.06	79.56 \pm 1.54
Citeseer	72.58 \pm 1.51	71.57 \pm 1.71	72.39 \pm 2.38
Pubmed	87.04 \pm 0.34	87.22 \pm 0.28	86.93 \pm 0.53
CORA-CA	82.36 \pm 0.72	82.19 \pm 2.61	81.71 \pm 1.42
DBLP-CA	90.83 \pm 0.25	91.98 \pm 0.18	90.72 \pm 0.23
Zoo	86.92 \pm 6.99	90.77 \pm 8.85	90.77 \pm 9.65
20newsW100	79.96 \pm 0.77	81.04 \pm 0.72	80.21 \pm 0.75
Mushroom	99.78 \pm 0.07	99.93 \pm 0.03	99.61 \pm 0.21
NTU2012	87.55 \pm 1.52	89.07 \pm 0.90	88.47 \pm 1.92
ModelNet40	98.27 \pm 0.21	98.18 \pm 0.12	98.41 \pm 0.11

D.3 Simplicial Higher-Order Datasets

Table 14 reports results introduced by Carrasco et al. (2025), a study conducted within the TopoBench framework, on real-world simplicial higher-order datasets. SCCNN achieves the highest overall performance, reaching 95.08% accuracy on the NAME classification task, while also maintaining strong performance across other metrics. Simplicial complex-based networks (SCN, SCCNN, SaNN, GCCN) consistently outperform standard graph methods (GCN, GAT, GIN), with SCCNN exhibiting particularly stable results, indicated by a low standard deviation of 0.56. These findings highlight the advantage of topological networks

in modeling higher-order tasks, where conventional pairwise graph structures fall short in capturing complex relational patterns.

Table 14: Higher-order datasets. Results are shown as mean \pm standard deviation. The best result is bold and shaded in grey, while those within one standard deviation are in blue-shaded boxes.

	Model	NAME (\uparrow)	ORIENT (\uparrow)	β_1 (\uparrow)	β_2 (\uparrow)
Graph	GCN	42.14 \pm 2.72	47.94 \pm 0.00	46.86 \pm 4.50	0.00 \pm 0.00
	GAT	18.09 \pm 0.65	47.94 \pm 0.00	7.45 \pm 0.05	0.00 \pm 0.00
	GIN	76.14 \pm 0.14	56.28 \pm 0.45	88.13 \pm 0.00	0.93 \pm 1.21
Simplicial	SCN	79.48 \pm 1.36	69.55 \pm 0.97	76.45 \pm 3.06	5.45 \pm 2.31
	SCCNN	95.08 \pm 0.56	86.29 \pm 1.23	90.20 \pm 0.20	65.82 \pm 2.70
	SaNN	81.76 \pm 1.37	61.65 \pm 0.55	88.46 \pm 0.09	39.22 \pm 2.80
	GCCN	86.76 \pm 1.27	76.60 \pm 1.67	84.20 \pm 4.80	41.82 \pm 20.19
	HOPSE-M	91.50 \pm 1.45	80.68 \pm 1.72	90.26 \pm 0.55	71.69 \pm 1.50
	HOPSE-G	81.75 \pm 1.26	62.17 \pm 0.98	88.28 \pm 0.08	35.37 \pm 2.25

Appendix E. Additional Dataset Details

To promote transparency, reproducibility, and ease of use, all dataset loading and preprocessing functionalities are encapsulated within the `TopoBench` library’s loader module (loader module). Most graph datasets are processed using the official `torch_geometric` loaders, which parse raw formats (e.g., `.csv`, `.npz`, or edge lists). The US-county-demos dataset is further adapted from the following repository (link). Higher-order hypergraph datasets are sourced from the repository of Chien et al. (2021) (link), while the MANTRA family datasets are adapted from (link) and integrated into `TopoBench` with consistent formatting adapted from `torch_geometric`, which stores the preprocessed datasets in the standardized PyTorch `.pt` files. This unified pipeline automates the full dataset preparation process and removes the need to access external repositories manually.

`TopoBench` includes all dataset licenses—where applicable—in the file located at the root of the repository and named `third_party_licenses.txt`. Additionally, a dedicated Datasets section in the `README.md` file provides references to the original source papers for each dataset included in the benchmark.

E.1 Graph datasets

Shared preprocessing: As emphasised in Appendix C.4—for demonstration purposes, only one fixed lifting is applied to transform graphs into each of the considered topological domains, leaving a domain-specific optimal lifting strategy beyond the scope of this paper. Specifically, a clique complex is used for simplicial lifting, cycle-based lifting is used for cellular domains, and k -hop lifting (with $k = 1$) is used for hypergraphs. Feature projection is also applied, where the $(n - 1)$ -cell features are multiplied by the corresponding incidence matrices to generate n -cell features.

Cora, Citeseer, and Pubmed are adapted from the open-source Planetoid dataset collection available in the `torch_geometric` repository (link to dataset). *Preprocessing:* no additional preprocessing is applied beyond the shared one.

MUTAG, PROTEINS, REDDIT-BINARY, IMDB-BINARY, IMDB-MULTI, NCI1, and NCI109 are sourced from the open-source TUDataset collection ([link to dataset](#)). *Preprocessing*: no additional preprocessing is applied beyond the shared one.

ZINC is adapted from the open-source dataset available at ([link to dataset](#)). *Preprocessing*: node features are first transformed into one-hot encodings, after which the shared preprocessing is applied.

Amazon Ratings, Minesweeper, Roman Empire, and Tolokers are obtained using the `HeterophilousGraphDataset` loader from `torch_geometric` ([link to dataset](#)). *Preprocessing*: no additional preprocessing is applied beyond the shared one.

The US-county-demos dataset is taken from the official Cornell website ([link to dataset](#)). *Preprocessing*: the version used is already preprocessed as in Jia and Benson (2020), and no further preprocessing is applied beyond the shared one.

E.2 Higher-Order datasets

Higher-order hypergraph datasets are acquired from the repository of Chien et al. (2021) ([link to dataset](#)) and adapted to the benchmark pipeline to conform to the integrated `torch_geometric` format used in TopoBench. Additional information regarding the hypergraph datasets is provided and discussed in Appendix D.1.

The code for the MANTRA family datasets is adapted from the (<https://github.com/aidoslab/MANTRA>) and integrated into TopoBench following the `torch_geometric` formatting.